

Tailored Porous Materials

Thomas J. Barton,[‡] Lucy M. Bull,[§] Walter G. Klemperer,^{*†} Douglas A. Loy,[◇] Brian McEnaney,[▽]
 Makoto Misono,[#] Peter A. Monson,[△] Guido Pez,[£] George W. Scherer,[♦] James C. Vertuli,[♥]
 and Omar M. Yaghi[≈]

RECEIVED

NOV 29 1999

OSTI

Department of Chemistry, Ames Laboratory, Iowa State University, Ames, Iowa 50011

*Materials Research Laboratory, University of California at Santa Barbara,
 Santa Barbara, California 93106*

*Frederick Seitz Materials Research Laboratory and Department of Chemistry,
 University of Illinois, Urbana, Illinois 61801*

Sandia National Laboratories, Albuquerque, New Mexico 87185

School of Materials Science, University of Bath, Bath BA27AY, United Kingdom

*Department of Applied Chemistry, Graduate School of Engineering, University of Tokyo,
 7-3-1 Hongo, Bunkyo-Ku, Tokyo 113, Japan*

*Department of Chemical Engineering, University of Massachusetts, Amherst, Massachusetts
 01003*

Air Products and Chemicals, Inc., 7201 Hamilton Boulevard, Allentown, Pennsylvania 18195

*Princeton University, Department of Civil Engineering and Operations Research, Princeton, New
 Jersey 08544*

Mobil Technology Company, Paulsboro Technical Center, Paulsboro, New Jersey 08066

Department of Chemistry and Biochemistry, Arizona State University, Tempe, Arizona 85287

[‡]Iowa State University. [§]University of California at Santa Barbara. Current address: Institut des Matériaux de Nantes, Laboratoire de Chimie des Solides, 44322 Nantes, France. ^{*}To whom correspondence should be addressed. [†]University of Illinois at Urbana-Champaign. [◇]Sandia National Laboratories. [▽]University of Bath. [#]University of Tokyo. [△]University of Massachusetts. [£]Air Products and Chemicals. [♦]Princeton University. [♥]Mobil Technology Company. [≈]Arizona State University.

Abstract

Tailoring of porous materials involves not only chemical synthetic techniques for tailoring microscopic properties such as pore size, pore shape, pore connectivity, and pore surface reactivity, but also materials processing techniques for tailoring the meso- and the macroscopic properties of bulk materials in the form of fibers, thin films and monoliths. These issues are addressed in the context of five specific classes of porous materials: oxide molecular sieves, porous coordination solids, porous carbons, sol-gel derived oxides, and porous heteropolyanion salts. Reviews of these specific areas are preceded by a presentation of background material and review of current theoretical approaches to adsorption phenomena. A concluding section outlines current research needs and opportunities.

Introduction

Porous materials have attracted the attention of chemists and materials scientists due to commercial interest in their application in chemical separations and heterogeneous catalysis as well as scientific interest in the challenges posed by their synthesis, processing and characterization. Application of basic scientific principles to the key technological issues involved has been difficult, however, and much more progress has been achieved in tailoring porous materials through manipulation of processing parameters than through understanding of the chemical and physical mechanisms that influence porosity. As a result, the tailoring of porous materials has proceeded largely in an empirical fashion rather than by design.

The present review is the product of a study panel convened under the auspices of the United States Department of Energy Council on Materials Research to assess basic research needs and opportunities in the area of tailored porous materials. Five classes of porous materials were selected for study that offer opportunities for tailoring their properties through rational design: oxide molecular sieves, porous coordination solids, porous carbons, sol-gel derived oxides, and porous heteropolyanion salts. In oxide molecular sieves, porosity can be tailored using either molecular or supramolecular templates to define both pore size and pore shape. Porous

DISCLAIMER

This report was prepared as an account of work sponsored by an agency of the United States Government. Neither the United States Government nor any agency thereof, nor any of their employees, make any warranty, express or implied, or assumes any legal liability or responsibility for the accuracy, completeness, or usefulness of any information, apparatus, product, or process disclosed, or represents that its use would not infringe privately owned rights. Reference herein to any specific commercial product, process, or service by trade name, trademark, manufacturer, or otherwise does not necessarily constitute or imply its endorsement, recommendation, or favoring by the United States Government or any agency thereof. The views and opinions of authors expressed herein do not necessarily state or reflect those of the United States Government or any agency thereof.

DISCLAIMER

Portions of this document may be illegible in electronic image products. Images are produced from the best available original document.

coordination solids offer the potential for a different type of tailoring, namely, the control of reactivity along pore walls through incorporation of different organic and inorganic functional groups. Unlike oxide molecular sieves and coordination solids, porous carbons are not crystalline materials and thus offer distinct advantages in terms of processibility, that is, tailoring on a macroscopic size scale to form membranes, monoliths, and fibers. Sol-gel derived oxides are also processible in this sense and can in addition be tailored on the molecular size scale. Porous heteropolyanion salts are unique relative to the other materials selected for study in that they are true molecular materials. Moreover, certain heteropolyanion salts have well-defined primary, secondary, and tertiary structures and as a result, porosity can be tailored on several different size scales in one and the same material. Treatment of these five systems is preceded by more general discussions of how porosity is defined and measured and how it can be understood and modeled on a fundamental level. A final section is also provided that outlines some of the challenges currently facing researchers in this area.

Background

Historically speaking, porous materials are defined in terms of their adsorption properties.¹ The term adsorption originally denoted the condensation of gas on a free surface as opposed to its entry into the bulk, as in absorption. Today, however, this distinction is frequently not observed, and the uptake of a gas by porous materials is often referred to as adsorption or simply sorption, regardless of the physical mechanism involved. Adsorption of a gas by a porous material is described quantitatively by an adsorption isotherm, the amount of gas adsorbed by the material at a fixed temperature as a function of pressure. The uptake of fluids into a porous material could be intuitively viewed simply as the filling of an existing vacuum ("Nature abhors a vacuum"²), but adsorption has long been recognized as a far more subtle phenomenon. J. W. Gibbs expressed the concept of adsorption on a general thermodynamic basis as follows. For the system of a fluid in contact with an adsorbent, he defined the amount adsorbed as the quantity of fluid that is in excess of that which would be present if the adsorbent had no influence on the behavior of the fluid.³ The

concept of adsorption as related to an area of exposed surface was developed by Irving Langmuir⁴ in his work on the “condensation” of gases on surfaces. From these studies emerged the concept of adsorption as a dynamic equilibrium between a gas and a solid surface resulting in a surface layer that is only one molecule thick, a concept that quite naturally led to the Brunauer, Emmett and Teller (BET) treatment of multi-layer adsorption.⁵ The BET equation is still commonly used for the determination of surface areas of porous solids.¹

Porous materials are most frequently characterized in terms of pore sizes derived from gas sorption data, and IUPAC conventions have been proposed for classifying pore sizes and gas sorption isotherms that reflect the relationship between porosity and sorption.⁶ Pores are classified according to pore diameter as follows: micropores have diameters less than about 2 nm; mesopores have diameters between 2 and 50 nm; and macropores have diameters greater than about 50 nm. Adsorption by mesopores is dominated by capillary condensation, whereas filling of micropores is controlled by stronger interactions between the adsorbate molecules and pore walls. It is noteworthy that this nomenclature addresses pore width but not pore shape, and pore shape can be important in some circumstances, such as when dealing with shape selective molecular sieve behavior. The IUPAC classification of adsorption isotherms is illustrated in Figure 1.⁶ The six types of isotherm are characteristic of adsorbents that are microporous (Type I), nonporous or macroporous (Types II, III and VI) or mesoporous (Types IV and V). The differences between Types II and III isotherms and between Types IV and V isotherms arise from the relative strengths of the fluid-solid and fluid-fluid attractive interactions: Types II and IV are associated with stronger fluid-solid interactions and Types III and V are associated with weaker fluid-solid interactions. The hysteresis loops usually exhibited by Types IV and V isotherms are associated with capillary condensation in the mesopores. The Type VI isotherm represents adsorption on nonporous or macroporous solids where stepwise multilayer adsorption occurs.

Reliable experimental methods are essential for characterizing tailored porous materials. Gas adsorption methods are commonly used,¹ as is mercury porosimetry,⁷ small angle X-ray scattering,⁸ fluid flow methods⁷ (permeation and diffusion), and thermoporometry.⁹ Optical and

electron optical methods are used for qualitative characterization and increasingly for quantitative analysis using image analysis methods.⁷ The advantages and limitations of the major characterization methods have been discussed elsewhere,^{1,7,8,9} and a thorough discussion is beyond the scope of this review. Three important points should be emphasized, however. First, most methods for obtaining pore size distributions model pores as arrays of non-intersecting cylinders or slit pores, whereas porous solids usually contain networks of interconnected pores. These methods assume that all pores are connected to the surface of the adsorbent and can drain in order of size, whereas in reality percolation effects play a key role in pore drainage.¹⁰ Second, microporous materials must be approached with caution: classical adsorption isotherms such as the BET equation are not applicable because of the strong adsorption forces in micropores resulting from the overlap of force fields from opposite pore walls. Consequently, adsorption in micropores occurs at very low pressures by a pore-filling mechanism. Exploration of this regime of the isotherm requires precise measurements of pressure and of amounts of fluid adsorbed, often at pressures less than 10^{-6} atm. In addition, microporous networks are often constricted, as in active carbons, and constrictions can cause molecular sieve action and activated diffusion at low temperatures. Activated diffusion poses problems when using N_2 adsorption at 77° K to characterize microporous solids. In such cases, adsorption of carbon dioxide at higher temperature has been used.¹¹ Finally, highly porous materials can be quite compliant, and this can present problems during characterization of the pore size distribution. Techniques such as mercury porosimetry, thermoporometry, and nitrogen desorption all exert stresses on the porous body, and in some cases the body contracts significantly during measurement such that pore size and volume are underestimated. For example, nitrogen desorption is a drying process where the pore liquid is nitrogen, and since the surface tension of liquid nitrogen at 77° K is 8.85 ergs/cm^2 ,¹² this results in large capillary stresses that can compress the solid network and cause the gel to shrink several-fold upon nitrogen desorption.^{13,14} The magnitude of the contraction can be calculated if the mechanical properties of the network are known, and the initial (undeformed) pore size and pore

volume can be estimated.^{14,15} Low pressure adsorption hysteresis has also been linked to the dimensional changes in porous solids that follow adsorption.¹⁶

Molecular Modeling of Adsorption Phenomena

Molecular modeling of fluid behavior in porous materials has been a very active area in recent years and substantial advances have been made.¹⁷ This has come about through a combination of progress in the fundamental statistical mechanics of inhomogeneous fluids and the widespread availability of high speed computing at low cost. A number of goals can be identified for the molecular modeling of adsorbed fluid behavior in the context of tailoring porous materials. These include: (i) formulation of microscopic mechanical models which give a physically correct description of the behavior of fluids in porous materials at the molecular level; (ii) development and application of methods for calculating equilibrium properties such as adsorption isotherms and/or dynamic properties such as diffusivities; and (iii) development of insights into microscopic behavior of fluids in porous materials and how this is reflected in experimental measurements of equilibria and dynamics as well as in the performance of the porous material in specific applications. Molecular models start with a picture of the microstructure of the porous material. This is then combined with a description of the intermolecular forces through which adsorbed molecules interact with the porous material and with each other. For some materials such as zeolites, a firm foundation for the microstructure is provided by experimental crystal structure determination. Zeolites are generally treated as collections of atoms and/or ions. The fluid-solid interactions are modeled with atom-atom potentials, possibly including electrostatic interactions in ionic materials. For other materials such as carbons and silica gels there is much more uncertainty in the microstructure, since these materials are intrinsically disordered. Porous carbons can be modeled as collections of slit pores with graphite-like surfaces with the pore-fluid potential treated with atom-atom potentials or integrated forms.^{3,18} Silica gels can be modeled as an agglomerations of microspheres of amorphous silica with the fluid-microsphere interactions treated with atom-atom potentials or integrated forms.¹⁹

Intermolecular Forces in Adsorption. Accurate determination of intermolecular forces in complex systems such as fluids in pores remains a largely unsolved problem. While it is true to say that we have a good qualitative understanding of these forces, accurate quantitative information is scarce. For bulk fluids, the most accurate intermolecular pair potentials are based on multiparameter functions with parameters obtained from experimental data from several different sources including second virial coefficients, molecular beam scattering, dilute gas transport properties and spectroscopy.²⁰ Far less information of this type is available for fluids in pores, where there is much more uncertainty in the functional form of the potential and values of the parameters involved. An important source of information about the fluid-solid interaction potential is experimental determination of the Henry's law constant which gives the limiting slope of the adsorption isotherm at low pressure.^{3,18} However, this property is very sensitive to nonuniformities in the adsorbent sample, and for microporous adsorbents the Henry's law regime often lies at extremely low pressures where adsorption measurements are especially difficult.

Treatments of intermolecular forces for fluids in pores start with atom-atom potentials between sites in the adsorbate molecule and sites in the adsorbent.^{3,18} In most cases these potentials are chosen to have the Lennard-Jones 12-6 form, following the widespread use of the site-site 12-6 potential as an effective pair potential in bulk fluids.²⁰ In addition, electrostatic interactions of the charge distribution in the adsorbent with permanent and/or induced charge distributions in the adsorbate molecules can be included. In the case of zeolites, for example, partial charges are often placed on the silicon, aluminum, and oxygen atoms of the framework in addition to the charge-balancing cations. For the adsorbate-adsorbate interactions, effective pair potentials from bulk fluid studies are usually used.

Statistical Mechanical Theories. Recent progress in the statistical mechanics of adsorption in pores has come principally from the recognition that the adsorbed fluid is inhomogeneous and the development of techniques for treating such inhomogeneous fluids. Foremost among these are the density functional theories.²¹ Such theories have provided a wealth of information about the nature of fluid behavior at free solid surfaces and in simple models

of pores such as slit pores and cylinders. Density functional theories have been especially successful in describing the nature of phase transitions of fluids in pores. Phenomena such as capillary condensation, wetting transitions and layering transitions are now much better understood through applications of density functional theory. These applications are well reviewed in articles by Evans.²¹ Since it provides a more accurate picture of fluid behavior in single pores than traditional methods such as the Kelvin equation, density functional theory has recently been used in conjunction with molecular simulations and pore size distributions as a characterization tool for porous materials.²² Density functional theory²³ has also been used to show that the slit pore model can generate all the six classes of adsorption isotherm in the IUPAC classification,⁶ as well as a seventh class of behavior called capillary drying in which the capillary transition occurs at a bulk pressure higher than the saturated vapor pressure. The variation of the adsorption isotherms with the strength of the fluid-solid interaction and wall separation in the slit pore model is illustrated in Figure 2.

Other recent applications of density functional theory have been to selective adsorption from mixtures²⁴ and the effect of confinement on liquid-liquid equilibrium.²⁵ Extension of the method to chain molecules in pores has also been made.²⁶ Most applications of density functional theory have been to simple pore geometries where the calculations involved can be reduced to one dimensional integrals. Recently, however an application to adsorption of xenon in zeolite NaA has been made²⁷ and work on more complex pore structures should be anticipated.

Molecular Simulations. Molecular simulation using the Monte Carlo and molecular dynamics techniques²⁸ is now the most widely used tool in the molecular modeling of fluid behavior in porous materials. This is especially true for complex materials such as zeolites where statistical mechanical theories are more difficult to apply.

Monte Carlo simulation in the grand canonical ensemble is the method of choice for studying equilibrium properties of fluids in porous materials and particularly for calculating adsorption isotherms. As an illustration of the kinds of calculations which are possible we focus on recent studies of adsorption in zeolites and related molecular sieve adsorbents. The focus of these studies

has been the development of intermolecular potentials as discussed above, calculation of the adsorption isotherm and heats of adsorption, and the development of insights into the molecular level behavior of the system. Two good examples are provided by calculations of adsorption of simple molecules in silicalite^{29,30} and some aluminophosphates.³¹ Interestingly, experimental data³² for argon in silicalite show a step in the adsorption isotherm indicative of a phase transition. This transition does not appear in the simulation results. The transition is thought to be a change in the silicalite structure induced by the presence of the argon, a conclusion supported by neutron diffraction studies³³ of the adsorbent structure at different points on the isotherm.

Monte Carlo simulations have also been used to study adsorption of mixtures³⁴ in porous materials. The focus of this work has been to understand the origins of selective adsorption and the nature of solution thermodynamics in porous materials. These studies are of fundamental importance in understanding the molecular basis of adsorption separations. Other areas where progress is being made in Monte Carlo simulations include more efficient sampling of high density states of fluids in the grand canonical ensemble via augmented/expanded ensemble methods³⁵ and configurational bias methods for studying chain molecules³⁶.

Molecular dynamics methods can be used to calculate transport properties in addition to thermodynamics. An important issue in adsorption is the nature of diffusive transport of molecules in porous materials.³⁷ Molecular dynamics makes it possible to track the details of the molecular motion in the system so that the mechanism of diffusion can be studied. Equilibrium molecular dynamics can be used to calculate the self diffusivity from the mean square displacement or the velocity autocorrelation function. A recent example of such a calculation is the work of June, *et al.*³⁸ who calculated the self diffusivities of methane and xenon in silicalite and obtained good agreement with the results from NMR measurements obtained for methane.^{39,40} The self-diffusivity is a measure of the diffusive motion of single molecules in the system at equilibrium. The transport diffusivity on the other hand is a measure of the collective motion of the fluid molecules in the presence of a concentration gradient. It is this quantity which is of importance in understanding transport effects in catalysis and separations. Maginn, *et al.*⁴¹ have used

nonequilibrium molecular dynamics to calculate the transport diffusivity for methane in silicalite. Other nonequilibrium molecular dynamics methods have been developed which allow the calculation of the transport diffusivity in the presence of large chemical potential gradients.⁴² Such methods hold considerable promise for improving our understanding of transport mechanisms in porous materials.

Oxide Molecular Sieves

Natural zeolites are crystalline aluminosilicate minerals that can be reversibly dehydrated without any apparent change in their crystalline forms.⁴³ The dehydrated minerals reversibly sorb water and methanol vapors, but largely exclude others, such as ether and benzene vapors. McBain regarded the zeolite mineral chabazite as an example of a "nearly perfect molecular sieve or a semi-permeable membrane of extremely regular structure,"⁴⁴ and today the family of oxide molecular sieves includes a wide variety of man-made microporous and mesoporous inorganic materials characterized by large internal surface area and pore volume.

Microporous zeolites constitute the largest known class of crystalline molecular sieves. These materials are composed of negatively charged aluminosilicate host frameworks that are sufficiently porous to accommodate a variety of different counterions plus, in many cases, guest molecules that can be reversibly desorbed. Zeolites have had enormous impact as catalysts and adsorbents in the chemical and petroleum industries.⁴⁵ The now classical example is the fluidized catalytic cracking (FCC) of hydrocarbons to gasoline by supported, rare-earth modified faujasite zeolite catalysts which have replaced the amorphous acid clay and synthetic alumina gel materials used previously.⁴⁶ It has been estimated that the use of this new technology has reduced the need for imported oil by 200 million barrels a year.⁴⁶ More recent major innovations have been in the use of ZSM-5 - based catalysts for the conversion of methanol to gasoline and also for the selective disproportionation of toluene into benzene and p-xylene.⁴⁷ Zeolites also have found large scale application as adsorbents and ion exchange agents. Most notably, certain lithium and calcium

faujasites exhibit N₂-selective adsorption properties and are useful for the separation of air,⁴⁸ and Zeolite 4A is widely used as a detergent builder.⁴⁹

Microporous zeolites and related crystalline oxides having a variety of micropore sizes and shapes are available, but crystalline mesoporous analogues are unknown. Two classes of ordered but noncrystalline mesoporous oxide molecular sieves are known, however. The first class, pillared layered solids, have been prepared from layered oxide materials by first separating the layers, then partially filling the space between the separated layers with inorganic pillars and finally removing the organic molecules thermally.^{50,51,52,53} Although many pillared layered oxides have been prepared for use as catalysts and adsorbents, these materials have failed to exhibit the narrow pore size distribution demonstrated by zeolites.^{54,55,56,57} More recently, a second class of mesoporous molecular sieves has been reported that contains uniformly-sized, cylindrical mesopores arranged regularly in an amorphous aluminosilicate matrix.^{58,59} This class of materials is discussed in more detail below.

Microporous and mesoporous oxide molecular sieves, characterized by large internal surface area and pore volume, form the backbone of many heterogeneous catalysts and separations media. The ability to tailor the pore size and shape of these porous materials would allow for control of the diffusion of both reagents and products into and out of the porous medium as well as control over the possible reaction intermediates that might form within the pore system. In short, tailoring of oxide molecular sieves implies control of size and shape selectivity in catalysis and separations. Tailoring of porosity in oxide molecular sieves in terms of *a priori* structural design has proved to be extremely difficult, however, due to the inherent complexity of the synthetic procedures employed. In general, oxide molecular sieves are prepared by hydrothermal synthesis methods which involve both chemical and physical transformations within an amorphous oxide gel, often in the presence of a template species.⁶⁰ The gel eventually crystallizes to form a material in which the template species and/or solvent molecules are guests within the channels and cages of an oxide host framework. A porous material is obtained upon removal of the guest molecules from the oxide framework. By varying the chemical composition of the gels, the reaction conditions, and

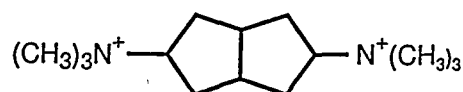
the templating agent it has been possible to arrive at the remarkable range of sieve compositions. The challenge of tailoring is largely the challenge of relating the initial synthesis conditions to the porosity of the molecular sieve material ultimately obtained.

Molecular Templates in Molecular Sieve Synthesis. The role of organic templates or structure-directing agents in zeolite synthesis has been widely discussed in the recent literature,⁶¹ and even though major strides have been made in the last decade towards understanding the self-assembly process, the goal of “synthesis by design” still remains largely elusive. Two factors complicate the understanding of zeolite synthesis. First, zeolites are often metastable products formed under kinetic rather than thermodynamic control, and different crystalline materials are often obtained under the same reaction conditions when different reaction times are employed.⁶² Recent experimental⁶³ and computational⁶⁴ studies have shown that microporous silica frameworks are less stable than quartz by only 7-14 kJmol⁻¹. Second, molecular templates are only one of many factors that control the structure of synthetic zeolites. Even though some clear examples of templating and structure-directing have been demonstrated, other systems show no such relationships and additional factors such as the influence of the temperature, pH, concentration, stirring rate, and the composition of the reaction vessel can be important.⁶⁵

Gies and Marler⁶⁶ were the first to comprehensively investigate the influence of the structure and chemical properties of organic and inorganic guest species on the synthesis of pure silica materials. Molecules with a similar shapes and volumes, regardless of their differences in chemical properties, formed the same types of silica framework structures in that globular guest molecules yielded cage frameworks, linear chain guest molecules yielded one-dimensional channel frameworks, and branched chain guest molecules yielded intersecting channel frameworks. Moreover, a linear correlation between the size of the guest and the size of the cages formed was observed. Gies⁶⁷ also showed by ¹³C solid-state NMR that the molecules were undergoing rapid reorientation within the cavities. This accounts for the insensitivity of the structures to the similarly sized, but chemically different, guest molecules. The kinetics of crystallization were affected by

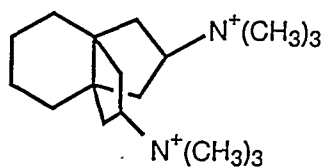
the basicity of the guest, but this was thought to be associated with the enhanced rate of silicate hydrolysis at higher pH's.

Zones, Olmstead and Santilli^{68,69} have shown both the scope and limitations of *a priori* design in their studies of SSZ-26 synthesis. Their aim was to produce a novel zeolite having a multidimensional channel system with large, 12-ring intersections. Realizing that the dication a



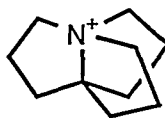
a

was used to synthesize ZSM-12, they introduced a fused cyclohexane ring into the structure to form the propellane b, a dication too large to be contained within the 1-dimensional ZSM-12



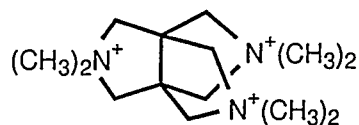
b

channel system, but potentially suited for occupying the junction of intersecting channels. Using this organic cation in a slightly aluminous reaction medium, a high silica zeolite (Si/Al=20-50), SSZ-26, was produced. The framework architecture of this zeolite consisted of intersecting 10- and 12-ring channels, with a propellane molecule trapped at each intersection.⁷⁰ SSZ-26 was not obtained, however, in the presence of monocationic propellane c or the structurally-related trication



c

d. Clearly, the geometry of the organic molecule is only one of many factors determining the



d

oxide framework structure in zeolites.

In theory, layered intermediates formed during zeolite synthesis could serve as precursors for pillared layered materials. These novel materials would be composed of layers having zeolitic microporosity and/or activity separated by mesoporous galleries. The first successful application of this concept was demonstrated by researchers at Mobil in the form of a material named MCM-36.^{71,72,73} Transmission electron micrographs of MCM-36 show that zeolite layers can be separated and pillared, using a silica source, to produce a pillared zeolite hybrid. Changes in the X-ray diffraction patterns, pore size distribution, and hydrocarbon sorption capacities support this proposed structure. The X-ray diffraction pattern of MCM-36 exhibits a low angle peak with a d-spacing of approximately 50 Å consistent with the interlayer separation observed in the transmission electron micrographs. In addition, those peaks assigned to the interlayer ordering are significantly broadened while those peaks assigned to the intralayer structure remained sharp and unaffected by the pillaring procedure. Pore size distribution measurements of MCM-36 exhibit an expected microporous component of 6-7 Å consistent with the zeolite pore structure as well as pores in the mesopore range between 30-35 Å. Surface areas and hydrocarbon sorption capacities increase by almost a factor of two compared to the parent un-pillared molecular sieve. Dynamic sorption data of a bulky hydrocarbon, 2,2-dimethylbutane, suggest the presence of a mesoporous channel system that makes the micropores more accessible.⁷³ The combination of the microporosity and activity of the zeolite layers and the mesoporous pillared structure should lead to applications involving larger molecules than those associated with traditional zeolitic materials.⁷⁴

Supramolecular Templates in Molecular Sieve Synthesis. A new class of mesoporous molecular sieves, M41S, has been discovered by extending the concept of zeolite templating with small organic molecules to longer chain surfactant molecules.^{58,59} Rather than individual molecular directing agents participating in the ordering of the reagents to form the porous material, assemblies of molecules, dictated by solution energetics, are responsible for the formation of these pore systems. This supramolecular directing concept (illustrated in Figure 3) has led to a family of materials whose structure, composition, and pore size can be tailored during synthesis by variation of the reactant stoichiometry, nature of the surfactant molecule, or by post-synthesis functionalization techniques.

The formation mechanism of this mesoporous family of molecular sieves is dictated by two features. The first is the dynamics of surfactant molecules to form molecular assemblies which lead to micelle and ultimately liquid crystal formation. The second is the ability of the inorganic oxide to undergo condensation reactions to form extended, thermally stable structures. The initial discovery involved the formation of silicates using alkyltrimethylammonium cationic surfactants in a basic medium. Subsequent efforts have shown these structures can also be formed in acid media^{75, 76} and by using neutral normal amines,⁷⁷ nonionic surfactants,⁷⁸ and dialkyldimethylammonium cationic surfactants.⁷⁹ In addition, several mechanistic studies have expanded the initial pathway studies to a more generalized view of an organic/inorganic charge balance driving force for the formation of these structures.^{75,76,77,80,81,82,83,84}

The initial members of the M41S family consisted of MCM-41 (hexagonal phase), MCM-48 (cubic Ia3d phase) and MCM-50 (a stabilized lamellar phase). MCM-41 exhibits an X-ray diffraction pattern containing three or more low angle (below $10^\circ 2\theta$) peaks that can be indexed to an hexagonal hk0 lattice.^{58,59} The structure is proposed to have an hexagonal stacking of uniform diameter porous tubes whose size can be varied from about 15 to more than 100 Å. An example of the characteristic X-ray diffraction pattern and proposed structure are shown in Figure 4. MCM-48, the cubic material, exhibits an X-ray diffraction pattern, shown in Figure 4, consisting of several peaks that can be assigned to the Ia3d space group. The structure of MCM-

48 has been proposed to be bicontinuous with a simplified representation of two infinite three-dimensional, mutually intertwined, unconnected network of rods as initially proposed by Luzzatti.⁸⁵ A more sophisticated and perhaps more realistic model⁷⁵ would be based on the concept of an infinite periodic minimal surface of the gyroid form, Q^{230} , proposed for water-surfactant systems.⁸⁶ A proposed structure is also shown in Figure 4. MCM-50, the stabilized lamellar structure exhibits an X-ray diffraction pattern consisting of several low angle peaks that can be indexed to $h00$ reflections. This material could be a pillared layered material with inorganic oxide pillars separating a two dimensional sheet similar to that of layered silicates such as magadiite or kenyaite as illustrated in Figure 4. Alternatively, the lamellar phase could be represented by a variation in the stacking of surfactant rods such that the pores of the inorganic oxide product would be arranged in a layered form.

Other M41S type mesoporous materials are: a cubic structure SBA-1 ($Pm3n$)⁸³ and SBA-2 (a three dimensional hexagonal structure, $p6_3/mmc$).⁸⁷ Further materials have been synthesized that are not as readily classified. These materials generally exhibit limited X-ray diffraction information (one peak) and may contain a random array of pores as shown in transmission electron micrographs. All of these mesoporous materials are characterized by having narrow pore size distributions comparable to microporous materials and extraordinary hydrocarbon sorption capacities (up to and equal to their weight).

The initial forms of the M41S family were synthesized as silicates and aluminosilicates. Subsequent synthesis efforts have produced materials having heteroatom substitution as well as nonsiliceous products. The initial nonsiliceous materials included oxides of W, Fe, Pb, Mo and Sb.^{82,83,88} Many of these materials exhibited very poor thermal stability and upon the removal of the template, the structures collapsed. Mesoporous zirconia and titania materials have been prepared, however, that exhibit satisfactory thermal stability and thus are believed to be composed of extended and complete oxide nets of the elements.^{89,90,91,92}

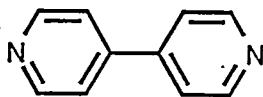
One of the unique features of the M41S family of materials is the ability to tailor pore size. The pore size can be varied from about 15\AA to more than 100\AA by varying the length of the alkyl

chain of the template molecule or by the use of auxiliary solubilized molecules.⁵⁹ A series of transmission electron micrographs of MCM-41 materials having pore diameters from 20-100 Å is shown in Figure 5. The approach taken to varying mesopore size in a regular, systematic fashion stands in stark contrast to the inability to accomplish such goals for traditional microporous zeolitic materials.

Finally, it should be noted that post-synthesis methods such as functionalization of pore walls can also affect the pore size in M41S materials. MCM-41 samples contain a large concentration of silanols which can be functionalized via simple elimination reactions. This post synthesis technique can be used to alter the pore size or affect the hydrophobicity of the pore wall. Alternatively, others species can be used to anchor moieties having specific catalytic or adsorptive properties.⁹³

Porous Coordination Solids

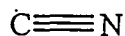
The construction of porous materials by linking transition metal ions with bridging ligands other than oxygen is an approach that offers much potential for the synthesis of new types of tailored porous materials.⁹⁴ The synthetic conditions and conceptual approach employed in their preparation differ from those usually employed in the synthesis of oxide molecular sieves. Porous coordination solids are prepared by combining solutions containing the appropriate organic ligands and metal ions at or near room temperature, and an attempt is made when designing their synthesis to exploit the directional nature of metal-ligand interactions for the construction of specific framework topologies. For example, Cu(I) ions are known to form tetrahedral complexes with organic ligands containing nitrogen donor atoms. Thus the addition of tetrahedral $[\text{Cu}(\text{CH}_3\text{CN})_4]^+$ as a PF_6^- salt to 4,4'-bipyridine (4,4'-bpy), e, a bifunctional building unit,



e

yields $\text{Cu}(4,4'\text{-bpy})_2\text{PF}_6$, as illustrated in Scheme 1.⁹⁵ Here, the cationic $\text{Cu}(4,4'\text{-bpy})_2^+$ framework defines a three-dimensional channel system in which PF_6^- counteranions reside. As is possible for many coordination solids, the structure of this framework can be related to that of cubic diamond by alternately replacing the C atoms and the C-C bond in the diamond structure with Cu(I) ions and the 4,4'-bpy ligands, respectively. In this fashion, an open framework is produced as a consequence of the large metric difference (8-8.5 Å) between the C-C bond and the 4,4'-bpy ligand. The use of molecular ligands for the construction of porous materials offers two important features favorable for tailoring both the porosity and the reactivity of coordination solids. First, the coordination chemistry of metal ions is extensive and well-established. This allows for numerous combinations of metal and ligand building blocks that can be manipulated at the molecular level in order to direct the assembly of a given target compound.⁹⁶ Second, the molecular building units tend to have good solubility and assembly reactions often proceed at room temperature. Consequently, the integrity of the component molecules is maintained in the coordination solid, and a close connection can frequently be established between molecular and solid state properties.

Anionic Frameworks. Metal cyanide compounds comprise a large family of coordination solids having anionic frameworks. The most thoroughly studied of these are the hexacyanometalates often referred to as Prussian blue analogues.^{97,98} Here, octahedral metal centers are linked together by the rod-like, doubly-bridging CN ligands, f, to generate three



f

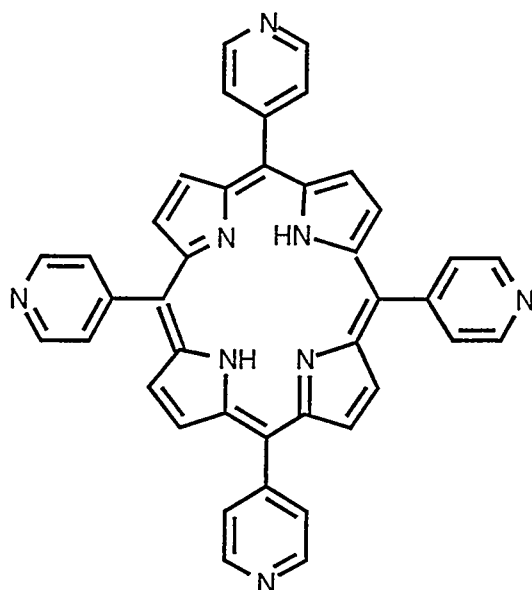
dimensional, cubic, anionic networks that are sufficiently porous to accommodate counteranions and/or additional neutral guest molecules. These guest molecules are in some cases coordinated to metal centers as in $\text{Mn}_3[\text{Co}(\text{CN})_6]_2 \cdot x\text{H}_2\text{O}$, which contains both uncoordinated “lattice water” and coordinated “ligand water.”⁹⁹ Many analogous materials have zeolitic properties in that they desorb water without degradation of the cyanometalate framework structure, and the resulting

porous materials can reversibly sorb a variety of small organic and inorganic molecules.¹⁰⁰

Related hexacyanometallates such as $M_2Zn_3[Fe(CN)_6]_2 \cdot xH_2O$, $M = K^+$, Na^+ , and Cs^+ , display similar behavior.¹⁰¹

Cationic Frameworks. Reaction of $AgNO_3$ with 4,4'-bipyridine (4,4'-bpy) under hydrothermal conditions yields colorless crystals of $Ag(4,4'-bpy)NO_3$. This cationic framework compound is composed of linear silver-bipyridine chains that are cross-linked by Ag-Ag bonds, $d_{Ag-Ag} = 2.98 \text{ \AA}$, to form three-fold interpenetrating, three-dimensional, three-connected α - $ThSi_2$ -like networks (see Figure 6).¹⁰² The nitrate counteranions occupy $23 \times 6 \text{ \AA}$ channels within this framework, and weak interactions between the nitrate anion and the cationic framework, $d_{Ag-O} = 2.78$ and 2.83 \AA , allow for anion exchange with ions such as PF_6^- , MoO_4^{2-} , BF_4^- and SO_4^{2-} .¹⁰² This exchange process is completed rapidly, without destruction of the metal-organic framework.

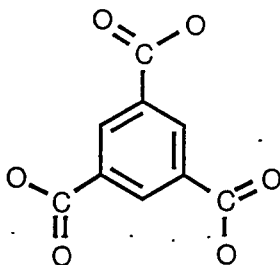
In the diamond-like, four-fold interpenetrated $Cu(4,4'-bpy)_2^+$ framework of $Cu(4,4'-bpy)_2PF_6$, the PF_6^- anions occupy a channel system nearly 6 \AA in diameter and can be exchanged with SCN^- ions.^{95b} Ion exchange is accompanied, however, by deformation of the cationic framework due to strong anion-framework interactions. A diamond-like network is also observed for the copper-tetracyanotetraphenylmethane framework in $Cu[C(C_6H_4CN)_4]BF_4 \cdot xC_6H_5NO_2$.¹⁰³ Here, framework interpenetration is not observed despite the presence of large, 22-\AA diameter channels in the $Cu[C(C_6H_4CN)_4]^+$ framework. These channels are occupied by stable clusters of BF_4^- anions and nitrobenzene solvent molecules that act as guests in the cationic framework and presumably inhibit interpenetration. Unfortunately, the orientation and number of guest species could not be determined X-ray crystallographically. A similar situation prevails in $Cu(tpp)(BF_4) \cdot xC_6H_5NO_2$ ($tpp = 5,10,15,20$ -tetra(4-pyridyl)-21H,23H-porphine, g). Here, a single, noninterpenetrated PtS-like network forms 15-\AA diameter channels that are occupied by BF_4^- and nitrobenzene molecules.¹⁰⁴



g

Neutral Frameworks. The crystalline cyanocobaltates $\text{Li}_3\text{Co}(\text{CN})_5 \cdot 3\text{DMF}$, $\text{Li}_3\text{Co}(\text{CN})_5 \cdot 1.42\text{DMF} \cdot 0.48\text{DMAC}$ (DMF = N,N-dimethylformamide and DMAC = N,N-dimethylacetamide), and $(\text{Bu}_4\text{N})_2[\text{Co}(\text{CN})_4(\text{NC}_5\text{H}_5)]$ are selective, high-capacity, reversible sorbents for O_2 .^{105,106,107} The first material shows a striking pressure reversible uptake of as much as ~ 55 cc O_2 per gram. Surprisingly, the compound is not microporous: O_2 is taken into the solid since it can bind to the coordinatively unsaturated Co(II) centers, but helium does not enter the crystal. Apparently, the $\text{Li}_3\text{Co}(\text{CN})_5 \cdot 3\text{DMF}$ structure is sufficiently flexible to accommodate the passage of O_2 to the Co(II) binding site.

Selective sorption of organic molecules containing specific functional groups has been observed for $\text{Zn}_2(\text{BTC})(\text{NO}_3) \cdot (\text{H}_2\text{O})(\text{C}_2\text{H}_5\text{OH})_5$, BTC = 1,3,5-benzenetricarboxylate (h),



prepared by diffusing triethylamine into a solution of 1,3,5-benzenetricarboxylic acid and zinc(II) nitrate hexahydrate in ethanol.¹⁰⁸ In this material, the $Zn_2(BTC)(NO_3)$ framework forms channels 14 Å in diameter that are occupied by water and ethanol. The nitrate ion is strongly bonded to the framework and cannot be exchanged. All of the neutral guest molecules can be exchanged at ambient temperature, however, including the three ethanol molecules that are coordinated to Zn(II). Exchange is quite selective for alcohols, and potential guest molecules such as tetrahydrofuran, methylcyclohexane, methylethylketone, acetonitrile, and acetone are excluded.¹⁰⁸ This selectivity appears to result from binding selectivity at the Zn(II) coordination site.

Selective sorption of aromatic organic molecules has been observed in a different type of BTC coordination solid, $Co[C_6H_3(COOH_{1/3})_3](NC_5H_5)_2 \cdot 2/3NC_5H_5$. As shown in Figure 7, this material has a layer structure where two pyridine molecules are coordinated to each cobalt center in a two-dimensional, planar Co-BTC network, with one pyridine molecule extending above the plane and the other below the plane.^{96c} These "anchored" pyridine molecules fail to fill the interlayer space, and as a result, uncoordinated pyridine molecules are intercalated between the Co-BTC layers. These guest molecules can be exchanged or even removed from the solid material with retention of the $Co[C_6H_3(COOH_{1/3})_3](NC_5H_5)_2$ host framework structure; this framework is stable up to 300 °C. Competitive sorption experiments performed using guest-free material show high selectivity for benzene derivatives. For example, benzonitrile is sorbed selectively from benzonitrile-acetonitrile mixtures. The probable origin of this selectivity is evident in Figure 7: ... favorable π - π stacking interactions between aromatic guest molecules that intercalate between the benzene rings of BTC units in adjacent layers.

Porous Carbons

Because of their disorganized microstructure, porous carbons cannot be tailored by control of crystal structure, as is the case, for example, with zeolites and coordination solids. However,

enough is known about the influence of processing on porosity in carbons to enable them, with care, to be tailored on a molecular level. This is best illustrated by the molecular selectivities of carbon molecular sieve membranes described below. An additional advantage of porous carbons is their processibility, that is, their ability to be fabricated into a variety of macroscopic forms more easily than many other porous materials.

Most industrial carbon materials are derived from organic precursors by heat-treatment in an inert atmosphere. During this carbonization process, a carbon residue is formed by condensation of polynuclear aromatic compounds and expulsion of side chain groups. However, industrial carbons retain a significant concentration of heteroelements, especially oxygen and hydrogen, and may also contain mineral matter. Carbons are broadly classified into graphitizing carbons that have developed three-dimensional graphitic order upon heat-treatment and non-graphitizing carbons that have not. A liquid phase is formed during carbonization of most graphitizing precursors in which polynuclear aromatic hydrocarbons are stacked into parallel arrays. This pre-graphitic, liquid crystalline material is called the carbonaceous mesophase. By contrast, cross-linking reactions occur during carbonization of non-graphitizing carbons that inhibit the development of a pre-graphitic structure.¹⁰⁹ Graphitizing carbons are predominantly macroporous, having significant pore volumes but low specific surface areas. These macropores are often relics of the microstructure of the precursor, e.g., cells in lignocellulosic materials or macerals in coals, or they may be manufacturing artifacts, e.g., gas bubbles or shrinkage cracks formed during carbonization.⁷ Non-graphitizing carbons are inherently microporous although some or all of the micropores may be closed.

The most important class of porous, non-graphitizing carbons is active carbons that have a high open porosity and high specific surface area, up to $1,200 \text{ m}^2 \text{ g}^{-1}$ in commercial active carbons. The major sources of active carbons are coals (lignites, bituminous coals, and anthracites), peat, wood and a wide range of organic byproducts of industry and agriculture. The adsorptive capacity of the carbonized materials is usually too low for practical applications, so porosity in the carbon is developed by activation during or prior to carbonization by reaction of the precursor either with

oxidizing gases such as H₂O or CO₂ or with other inorganic chemical activating agents such as H₃PO₄ or ZnCl₂. About 90% of active carbons are produced in granular or powder form, with most of the remainder in pelleted form. About 80 wt % of active carbons are used for liquid phase applications such as water treatment, decolorization, foods and pharmaceuticals, chemicals, and mining. The remainder are used for gas phase applications in solvent recovery, air purification, gasoline recovery, catalysis, gas separation, and cigarette filters, and military and nuclear applications.

Mechanisms of activation by reaction with oxidizing gases during carbonization have been extensively studied. In the initial stages of activation, new open micropores are created, possibly by removal of secondary carbon formed by cracked volatiles from pore entrances. In the later stages of activation micropore widening is the dominant process so that the pore size distribution extends into the mesopore size range.¹¹⁰ Much less is known about mechanisms of chemical activation although there has been recent work on the chemical activation of woods and coals by phosphoric acid.^{111,112,113} Measurable open porosity develops upon heat treatment of wood with phosphoric acid at 200°C, increases to a maximum of *ca.* 2,000 ²g⁻¹) at 350-500°C and decreases at higher heat-treatment temperatures. Studies by ¹³C NMR have shown that phosphoric acid promotes cross-linking reactions and dehydration at low temperatures, thus bonding otherwise volatile material into the structure and leading to increased carbon yield. Partial depolymerisation of lignin and hemicellulose also occur, cellulose being more resistant to depolymerization. It is inferred that generation of accessible porosity results from dilatation following depolymerization. At higher temperatures (*ca.* 450°C) there is repolymerization and a sudden growth in the average size of aromatic clusters, indicating that bond cleavage and structural rearrangement occur, causing contraction and the observed reduction in porosity.

Table 1¹⁴ shows how the distribution of different pore types in active carbons varies with the nature of the precursor. By judicious choice of the precursor and by careful control of carbonization and activation it is possible to tailor active carbons for particular applications. Carbons used for liquid phase applications require significant mesoporosity as provided by the

lignite-based active carbon (see Table 1) and also by phosphoric acid activated wood-based carbons. Highly microporous carbons are required for gas phase applications.

Non-graphitizing carbons such as active carbons have a very disordered structure as revealed by high resolution electron microscopy,¹¹⁵ and various model structures have been proposed. Although the models differ in detail, the essential feature of all of them is a twisted network of defective hexagonal carbon layer planes, cross-linked by aliphatic bridging groups. The width of layer planes varies, but typically is about 5 nm. Simple functional groups (e.g., C-OH, C=O) and heteroelements are incorporated into the network and are bound to the periphery of the carbon layer planes. Functional groups can have an important influence on adsorption. In active carbons the layer planes occur singly or in small stacks of two, three, or four with variable interlayer spacings typically in the range 0.34 to 0.8 nm. There is considerable microporosity in the form of an interconnected network of slit-shaped pores formed by the spaces between the stacks. Thus the widths of pores formed by interlayer spacings are significantly less than 2 nm, the upper limit for micropore widths. Constrictions in the microporous network are particular features of the structure that control access to much of the pore space. Constrictions may also occur due to the presence of functional groups attached to the edges of layer planes and by carbon deposits formed by thermal cracking of volatiles. The high adsorptive capacity of active carbons used in gas adsorption mainly results from the presence of small micropores (ultramicropores or nanopores) of width commensurate with adsorbate molecules. In such pores there is overlap of the force fields from opposite pore walls leading to strong adsorption.

Carbon molecular sieves, CMS, can be prepared by deposition of carbon from the vapor phase, CVD.^{116,117,118} CMS are used in tonnage quantities to separate N₂ from air by pressure swing adsorption.¹¹⁹ The separation is kinetic, depending upon faster adsorption of the smaller O₂ molecule ($\sigma = 0.346$ nm) into micropores than the larger molecule N₂ ($\sigma = 0.364$ nm). CMS show little selectivity between O₂ and N₂ at equilibrium. The kinetic selectivity of a CMS for separation of O₂ and N₂ is shown in Figure 8. It has been presumed that selectivity results from constriction of apertures in the microporous network by CVD. However, recent work shows that reduction in

particle size of CMS by grinding progressively reduces $O_2:N_2$ selectivity.¹²⁰ The authors speculate that CMS consist of non-selective active carbon particles (5-20 μm) that are contained in $\sim 150 \mu\text{m}$ domains enclosed by a size-selective CVD coating that is destroyed by grinding. There is a need for better sieves that retain a high $O_2:N_2$ selectivity but with higher O_2 capacity; CMS that show an equilibrium selectivity for O_2 versus N_2 would also be desirable.

CMS membranes show high selectivity between hydrogen and C_1 - C_4 hydrocarbons. Illustrative selectivity factors^{119,121} are given in Table 2 which show, counter to intuition, that permeabilities of the hydrocarbons are higher than that of H_2 and that they increase with molecular weight. This is because under the conditions used the transport processes in the CMS pores are dominated by surface flow of the most strongly adsorbed components in the adsorbed phase, i.e., the highest hydrocarbons. The processes involved are illustrated in Figure 9. This study illustrates how selectivity can result from a subtle interplay between different processes.¹²² In the case illustrated in Figure 9 and Table 2, selectivity in the smallest pores results from size exclusion. In larger pores of width ~ 2 molecular dimensions, surface diffusion dominates under conditions where adsorbed phase concentrations are high. For larger pores of width $> 5 \text{ nm}$, non-selective viscous flow is the principal transport mechanism. However, Knudsen diffusion dominates transport processes at high temperatures. Clearly, there is much scope for developing CMS membranes with different pore sizes and operating them at different temperatures in order to achieve a wider range of selectivity than is possible today. Modeling these complex processes is also a rich field for molecular simulation studies.

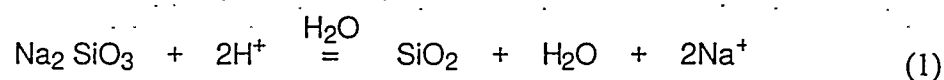
Active carbon fibers, ACF, can be prepared by carbonization and activation of a range of polymer fibers (e.g. phenolics, acrylics and vinyls) and isotropic pitch fibers.¹²³ ACF are usually microporous, although mesoporous fibers are also known. They are characterized by rapid diffusion of adsorbates into and out of the fibers. Textile technology has been adapted to produce a range of flexible woven and non-woven forms of ACF that have found a diverse range of applications such as water and air purification, military clothing, surgical dressings, and high capacity double layer capacitors. Rigidized monolithic forms of ACF called carbon bonded carbon

fibers, CBCF, have been produced from a slurry of chopped carbon fibers and a resin powder that is filtered to produce a mat. This is followed by carbonization of the resin binder and activation of the fiber.¹²⁴ One form of CBCF has exhibited molecular sieve character, showing selectivity between CO₂ and CH₄. An interesting aspect of this study is the use of an electric field across the CBCF to assist desorption of CO₂. ACF and related materials are promising materials for electrosorption and thermal swing processing using resistive heating, although their potential has not been fully explored.

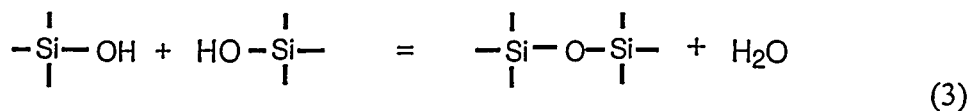
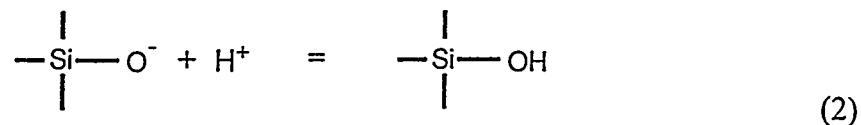
There is much current interest in the development of porous carbon anodes for Li ion batteries.^{125,126,127,128,129} The capacity of commercial carbon anodes is 200-250 mAhg⁻¹, but laboratory studies have shown that carbons with capacities in the range 500-900 mAhg⁻¹ can be prepared. The nature of the interaction of Li⁺ ions with carbons depends upon microstructure. Lithium intercalates into graphitic carbons, the extent of staging increasing with graphitic character. For non-graphitizing carbons, lithium is bound close to carbon layer planes, possibly in micropores. For carbons heat treated to less than 1000 °C, Li is bound close to residual H in the carbon structure. An interesting form of porous carbon anode of high capacity (925 mAhg⁻¹) has been produced by carbonizing organics inserted into the pores of a pillared clay.^{130,131,132}

Sol-Gel Derived Oxides

Amorphous silica can be prepared by acidification of basic aqueous silicate solutions as in reaction (1), and when reaction conditions are properly adjusted, porous silica gels are

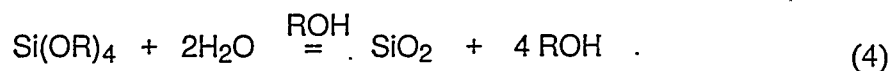


obtained.¹³³ Two types of chemical reactions are involved: silicate neutralization producing silicic acids, reaction (2), followed by condensation polymerization of the silicic acids, reaction (3).

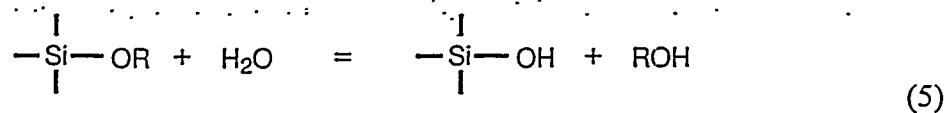


If water is evaporated from the pores of silica hydrogels prepared in this fashion, porous xerogels (dried gels) are obtained. Porous, amorphous oxides of silicon and other elements are produced in this fashion commercially on a very large scale and have found widespread application as high surface area catalysts, catalyst supports, chromatographic stationary phases, and gas sorbents.^{134,135} As hydrophilic materials, their sorption properties complement those of porous carbons, since carbons are hydrophobic and tend to selectively adsorb hydrocarbons.

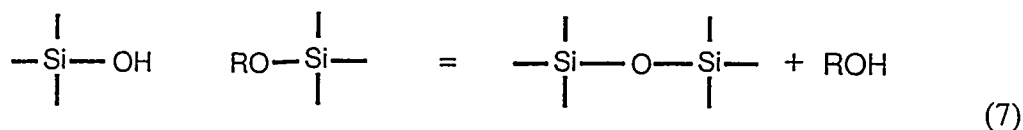
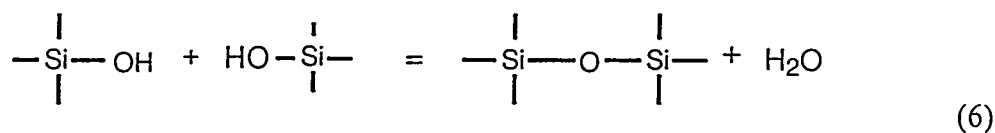
An alternative route to porous, amorphous oxides involves reaction of alkoxides with water as illustrated in reaction (4) for silica.^{136,137} Here, silicic acids are first produced by hydrolysis of a



silicon alkoxide, formally a silicic acid ester, as in reaction (5). The silicic acids thus formed can



then either undergo self-condensation, reaction (6), or condensation with an alkoxide as in reaction (7). The overall reaction therefore proceeds initially as a condensation polymerization reaction to



form soluble, high molecular weight polysilicates (a sol), and these polysilicates then link together to form a three-dimensional network whose pores are filled with solvent molecules (a gel). Hence the name “sol-gel polymerization” of alkoxides and “sol-gel processing” of oxides.

Both sol-gel derived oxides and oxide molecular sieves are usually prepared from oxide gels, and in a certain sense both can be regarded as sol-gel derived oxides differing only in their degree of structural ordering. In sol-gel derived oxides, neither the oxide framework nor the pore structure are ordered. Mesoporous oxide molecular sieves resemble sol-gel derived oxides in that they have noncrystalline, amorphous oxide frameworks but differ in that their mesopores are uniform and ordered. Microporous oxide molecular sieves also have uniform, ordered pore structures but in addition have crystalline oxide frameworks. Ordering is achieved in the synthesis of oxide molecular sieves by heat treatment of an oxide gel in the presence of an organic or inorganic "structure-directing" species. This heat treatment promotes reversible dissolution of the solid oxide gel framework into pore fluid solution and subsequent nucleation and growth of ordered materials. In short, heat treatment allows the system to approach metastable equilibrium. Note that the true equilibrium state for most oxides is a dense, nonporous phase and that oxide molecular sieves as well as sol-gel derived oxides are thermodynamically metastable phases. In both cases, optimized processing conditions represent a balance between kinetic and thermodynamic factors.

Sol-gel derived oxides have yet to receive widespread application as porous materials, but they have nonetheless been investigated extensively due to the versatility of sol-gel processing techniques. Sol-gel processing conditions can be employed in the fabrication of oxide monoliths, fibers, thin films, and monodisperse powders.^{136,137} Moreover, the chemical properties of sol-gel derived oxides can be manipulated by incorporating organic, organometallic, and inorganic functional groups into the gel framework.¹³⁸ The discussion that follows is restricted almost exclusively to sol-gel derived silica, but the principles involved are quite general and can be applied to the processing of many other main group and transition metal oxides. In the first section, the influence of processing conditions on porosity is considered in terms of the distinct processing steps involved. The two sections that follow are concerned with tailoring the porosity of sol-gel derived oxides not through manipulation of processing conditions but instead through manipulation of precursor composition and geometry.

Sol-Gel Processing. The initial stages of sol-gel processing proceed in solution, and the porosity of the final product is most easily tailored during these initial stages by introducing acids such as hydrochloric acid or bases such as ammonium hydroxide into the reaction solution. Silica xerogels processed under relatively acidic conditions display Type I nitrogen sorption isotherms characteristic of microporous materials whereas those processed under basic conditions display Type IV isotherms characteristic of mesoporous materials (see Figure 1).¹³⁹ These types of isotherms represent extremes in behavior, and by varying the amount of acid or base added to the reaction solution it is possible to prepare xerogels that display Type I/Type IV composite isotherms reflecting the presence of both micro- and mesoporosity. Transmission electron microscopic studies show that the microstructure of xerogels varies from homogeneous to particulate as the processing conditions are varied from acidic to basic.¹⁴⁰ Studies of particulate silica xerogels obtained from aggregated aqueous silica colloidal sols and studies of silica nanoparticles prepared by controlled hydrolysis of tetramethylorthosilicate both show that mesoporosity arises from interstitial pore space in particle aggregates and as a result, the average mesopore radius increases with increasing particle size.¹⁴¹ This observation supports the idea that porosity in sol-gel derived

oxides depends on the internal structure of the primary particles, the size and size distribution of the primary particles, how these primary particles aggregate, and how the gel structure responds to the capillary stresses during drying (see below).

Quasielastic light scattering (QELS) has proved to be a powerful tool for monitoring the course of sol-gel polymerization in solution since the Z-average hydrodynamic radius R_h of the polysilicates formed can be continuously monitored as a function of time. For sol-gel polymerization of dilute $\text{Si}(\text{OCH}_3)_4$ in basic methanol solution, an extended growth stage is observed where R_h varies exponentially with time.¹⁴² Exponential growth of this type is characteristic of particle aggregation processes controlled by chemical kinetics (reaction-limited cluster aggregation) as opposed to particle diffusion (diffusion-limited cluster aggregation).¹⁴³ For sol-gel polymerization of dilute $\text{Si}(\text{OCH}_3)_4$ in basic methanol solution, this stage begins when R_h is about 5 nm. A comparison between sol-gel polymerization under basic and acidic conditions has been made in a slightly more concentrated system.¹⁴⁴ Under basic conditions, exponential growth was observed once the hydrodynamic radius reached about 20 nm but under acidic condition, R_h was <2 nm at the onset of the exponential growth stage. In both cases, the exponential growth stage was preceded by a shorter, faster initial growth stage and was followed by a critical growth stage. During this critical growth stage, R_h diverges as the gel time t_{gel} is approached according to $R_h = (t_{\text{gel}} - t)^{-\gamma}$. In summary, QELS studies have shown that the sol-gel polymerization of $\text{Si}(\text{OCH}_3)_4$ proceeds in three successive, possibly overlapping polymerization stages: (1) initial polymerization of the $\text{Si}(\text{OCH}_3)_4$ precursor into polysilicates that serve as monomers in the second stage, (2) exponential growth of polysilicate primary particles formed in the first stage into particle aggregates that serve as monomers in the final stage, and (3) critical growth of the aggregates formed in the second stage into a gel.

Qualitative comparison of the gas sorption data, electron microscopic information, and quasielastic light scattering data just reviewed strongly suggest that micro- and mesoporosity in sol-gel derived xerogels is ultimately derived from the size of primary particles formed during the early stages of sol-gel polymerization. Under more basic conditions where larger primary particles

are formed, mesoporosity is obtained, and under more acidic conditions where smaller primary particles are formed, microporosity is obtained. Two points should be noted in this context, however. First, the preceding discussion has focused on the influence of acidic and basic conditions on porosity, but many other processing conditions play a subsidiary but important role.^{133,136} Second, acidic and basic conditions affect not only the sizes but also the structures of the primary particles formed in the course of sol-gel polymerization. The polysilicate primary particles formed under basic conditions are more cross-linked than those formed under acidic conditions and are therefore more dense as well.¹⁴⁵

At the moment of gelation, significant concentrations of soluble silicates are still present in the liquid phase. During the next stage of sol-gel processing, gel aging, these species become attached to the gel network, leading to an increase in its rigidity. In addition, condensation can still occur within the gel network according to reactions (6) and (7), resulting in stiffening and contraction (syneresis).¹⁴⁶ This type of network stiffening can be enhanced by adding alkoxide monomer after gelation.¹⁴⁷ Such treatments cause some modification of the pore structure in the wet gel, but their most important effect is a strengthening of the gel network that serves to reduce the amount of shrinkage that occurs during drying. The pore size distribution can be systematically altered by aging in an reactive liquid that promotes equilibration in the gel framework: dissolution/precipitation transfers material from the surfaces of larger pores to smaller ones, leading to coarsening. Aging by dissolution/precipitation raises the modulus of a gel initially, as material is deposited in regions of negative curvature. Longer aging can reduce the rigidity, however, probably owing to instability in long chains that breaks up the network.¹⁴⁸

Once gel aging is completed, steps are taken to remove the liquid phase from the solid gel framework. Drying of gels involves shrinkage, implying as much as an order of magnitude reduction in pore volume and a corresponding reduction in pore sizes.¹⁴⁹ The final density depends on the balance between the capillary pressure that drives shrinkage and the rigidity of the network that resists shrinkage.¹⁵⁰ If the connectivity of the network of the gel is low, the gel may be so compliant that the pores collapse^{151,152} By minimizing the degree of crosslinking in the

gel, the network can be made supple enough to collapse until the "pore" diameter is determined by the size of the solvent molecule.¹⁵³ On the other hand, some gels undergo large contraction during drying, but then spring back completely. This is achieved by passivating the surfaces of the gel through trimethylsilylation of hydroxyl groups with trimethylchlorosilane, so that branches of the network cannot bond to one another when they are forced into contact during drying.^{154,155}

The final stage of sol-gel processing is a heat treatment stage. As a gel is heated in air, adsorbed solvent evaporates and by about 400 °C, most organics burn off. In some cases, when small molecules or substituents are removed from within the dried gel framework, micropores are created and the surface area increases.¹⁵⁶ As the temperature approaches the glass transition temperature of the network, sintering results from viscous flow driven by the curvature of the solid/vapor interface.¹⁵⁷ This causes the smallest pores to collapse first, followed by larger pores. Thus, micropores can be created by heating at low temperatures, and they can be eliminated by partial sintering. Many gels crystallize when heated, even at temperatures too low for significant sintering. In such cases, crystals grow within the porous network, and the pores engulfed within the crystal grains are very difficult to eliminate by subsequent heat treatment. However, the sintering rate accelerates monotonically with temperature, while the crystallization rate goes through a maximum at a temperature well below the melting point, so the competition between sintering and crystallization can be tilted in favor of sintering by using rapid heating.¹⁵⁸ Quantitative prediction of the thermal history needed to obtain densification before crystallization requires knowledge of the nucleation and growth rates within the gel matrix; unfortunately, very little is known about the mechanisms of nucleation and growth in gels.

The Molecular Building Block Approach. Sol-gel derived oxides can be tailored on a macroscopic size scale since gelation, aging, and drying can usually be achieved with retention of the overall macroscopic shape assumed by the material upon gelation, be it a fiber, a thin film, or a monolith. Tailoring on a microscopic size scale is far more difficult since these materials are structurally disordered on the molecular size scale. Oxide molecular sieves, on the other hand, can be tailored on the microscopic size scale in terms of micro- and mesoporosity (see above) but are

virtually impossible to tailor on the macroscopic size scale due to their crystallinity. The molecular building block approach to sol-gel derived oxides^{159, 160} combines the advantages associated with traditional sol-gel derived oxides and oxide molecular sieves by tailoring properties on both the microscopic and macroscopic size scales. In this approach, sol-gel processing techniques are employed to polymerize molecular oxide alkoxides designed to influence the properties of the sol-gel derived material much in the same way that monomers employed in organic polymerizations are designed to influence the properties of the resin or polymer obtained. For example, porous materials require mechanically rigid framework structures, and precursor molecules containing mechanically rigid core structures are in principle suitable molecular building blocks for this type of extended framework. Specifically, the $[\text{Si}_8\text{O}_{12}](\text{OCH}_3)_8$ precursor molecule¹⁶¹ has a rigid $[\text{Si}_8\text{O}_{12}]$ cage core structure, and the $[\text{Ti}_{16}\text{O}_{16}](\text{OC}_2\text{H}_5)_{32}$ precursor molecule¹⁶² has $[\text{Ti}_{16}\text{O}_{16}]$ core structure where oxygen atoms are closest-packed and titanium atoms occupy octahedral interstices. The influence of the molecular building block employed extends beyond the local structure of sol-gel derived oxides, however, since the nature of the molecular precursor also influences the molecular growth pathway followed during sol-gel polymerization. In traditional sol-gel processing, porosity can be tailored by manipulating the size distribution and structure of the primary particles formed by hydrolysis/condensation of simple alkoxides, but since a variety of different primary particles is formed regardless of the processing conditions employed, pore size distributions and pore shapes can be only crudely tailored at the molecular level. In the molecular building block approach, a single molecular entity can serve as the primary particle during sol-gel polymerization, and as a result, the meso- and microstructural homogeneity of sol-gel derived oxides can be tailored.

A necessary condition for successful implementation of the molecular building block approach is stability of the molecular building block employed under sol-gel processing conditions. If the molecular structure of the precursor molecule employed is to influence the porosity of the sol-gel derived oxide ultimately obtained, the core structure of the precursor molecule must remain largely intact in the final product. The issue of molecular building block stability was first explored in a

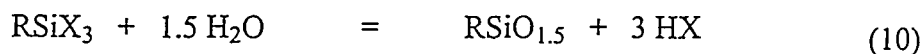
comparative study of $\text{Si}(\text{OCH}_3)_4$ and $[\text{Si}_8\text{O}_{12}](\text{OCH}_3)_8$ sol-gel polymerization. During the early stages of sol gel processing, hydrolysis of $\text{Si}(\text{OCH}_3)_4$ and condensation of the resulting SiOH groups yields a family of low molecular weight polysilicates that have been identified using gas chromatography coupled with mass spectrometry (see Figure 10).^{163, 164, 165} None of these low molecular weight polysilicates were observed upon hydrolysis/condensation of $[\text{Si}_8\text{O}_{12}](\text{OCH}_3)_8$, nor were any of the Si - O - Si siloxane bonds in the $[\text{Si}_8\text{O}_{12}]$ core of $[\text{Si}_8\text{O}_{12}](\text{OCH}_3)_8$ or its hydrolysis products attacked under these conditions.¹⁶¹ Comparative ^{29}Si MAS NMR studies of $\text{Si}(\text{OCH}_3)_4$ - derived and $[\text{Si}_8\text{O}_{12}](\text{OCH}_3)_8$ - derived xerogels gave evidence for a barely measurable amount of cage degradation in the $[\text{Si}_8\text{O}_{12}](\text{OCH}_3)_8$ - derived material, suggesting that the cubic Si_8O_{12} core was largely intact in the final material.¹⁶⁴ As expected, the properties of $\text{Si}(\text{OCH}_3)_4$ - derived and $[\text{Si}_8\text{O}_{12}](\text{OCH}_3)_8$ - derived xerogels were quite different, with apparent BET surface areas of 510 and 919 m^2/g , respectively, when the materials were processed under similar conditions.¹⁶⁶ These differences in porosity could be interpreted structurally from transmission electron micrographs of platinum replicated xerogels of the type shown in Figure 11, where silica appears as a white image against a black background. Micrographs obtained from replicas of $[\text{Si}_8\text{O}_{12}](\text{OCH}_3)_8$ - derived xerogels (see Figure 11a) show uniformly sized silica structures and pores relative to the broader size distribution of silica structures and pores in micrographs of replicas obtained from $\text{Si}(\text{OCH}_3)_4$ - derived xerogels (see Figure 11b). Moreover, the silica features observed in micrographs of $[\text{Si}_8\text{O}_{12}](\text{OCH}_3)_8$ - derived xerogels are on the average thicker than the corresponding features in micrographs of $\text{Si}(\text{OCH}_3)_4$ - derived xerogels. The electron micrographs therefore support a model for $[\text{Si}_8\text{O}_{12}](\text{OCH}_3)_8$ sol-gel polymerization where polymers of the structurally rigid cubic precursor are themselves rigid relative to $\text{Si}(\text{OCH}_3)_4$ - derived polymers and therefore undergo less cyclization and crosslinking during all stages of sol-gel processing, ultimately yielding more uniformly-sized silica structures and pores in the xerogel. In the case of $\text{Si}(\text{OCH}_3)_4$ - derived xerogels, smaller silica structures are not observed as the result of using a smaller molecular building block. Instead, the conformational flexibility of $\text{Si}(\text{OCH}_3)_4$ -

derived polysilicate chains allows for extensive cyclization and leads to the observed clustering of silicate chains into larger and more irregularly-shaped silica structures.

The role played by molecular building blocks as primary particles during the exponential growth stage of sol-gel polymerization has been explored in the titania system, where stable molecular building blocks are available that are considerably larger than those available in the silica system and thus more amenable to study using dynamic light scattering. In the titania system, the course of titania sol-gel polymerization can also be monitored using ^{17}O NMR spectroscopy in solution and the solid state due to the large, >400 ppm chemical shift range observed for oxygen nuclei in titanates. The most extensive study completed to date involved comparison of $\text{Ti}(\text{OC}_2\text{H}_5)_4$ and $[\text{Ti}_{16}\text{O}_{16}](\text{OC}_2\text{H}_5)_{32}$ sol-gel polymerization. Markedly different ^{17}O NMR spectra were observed for $\text{Ti}(\text{OC}_2\text{H}_5)_4$ - derived and $[\text{Ti}_{16}\text{O}_{16}](\text{OC}_2\text{H}_5)_{32}$ - derived xerogels, and these differences could be interpreted structurally using ^{17}O selective labeling techniques.¹⁶⁷ This ^{17}O NMR study showed that the oxide oxygen centers in the $[\text{Ti}_{16}\text{O}_{16}]$ core structure of the $[\text{Ti}_{16}\text{O}_{16}](\text{OC}_2\text{H}_5)_{32}$ precursor could be observed intact in the xerogel obtained. Nitrogen sorption measurements using xerogels prepared from $\text{Ti}(\text{OC}_2\text{H}_5)_4$ and $[\text{Ti}_{16}\text{O}_{16}](\text{OC}_2\text{H}_5)_{32}$ under the same acidic processing conditions displayed Type IV and Type I isotherms, respectively. Although a Type IV isotherm was observed for $\text{Ti}(\text{OC}_2\text{H}_5)_4$ - derived gels, BET plots failed to show linearity even in the $0.001 < p/p_0 < 0.05$ region, indicating significant microporosity. The isotherm is therefore more appropriately described as a Type I/Type IV composite isotherm. The narrower pore size distribution observed for $[\text{Ti}_{16}\text{O}_{16}](\text{OC}_2\text{H}_5)_{32}$ - derived xerogels relative to $\text{Ti}(\text{OC}_2\text{H}_5)_4$ - derived xerogels can be understood in terms of primary particle size distributions during the sol-gel polymerization stage. Quasielastic light scattering data indicate very different types of growth kinetics for the two systems, with $\text{Ti}(\text{OC}_2\text{H}_5)_4$ polymerization showing an initial growth stage followed by an exponential growth stage, but $[\text{Ti}_{16}\text{O}_{16}](\text{OC}_2\text{H}_5)_{32}$ polymerization showing initial exponential growth with no evidence of an earlier growth stage.¹⁶⁸ Moreover, plots of the Z-average hydrodynamic radius R_h as a function of time show an average primary particle size of 75 to 100 nm for $\text{Ti}(\text{OC}_2\text{H}_5)_4$ polymerization but < 5 nm for $[\text{Ti}_{16}\text{O}_{16}](\text{OC}_2\text{H}_5)_{32}$ polymerization. The

$[\text{Ti}_{16}\text{O}_{16}](\text{OC}_2\text{H}_5)_{32}$ precursor and its hydrolysis products serve as primary particles during the exponential growth stage and produce a xerogel whose pore size approximates its 1-2 nm molecular diameter. In contrast, $\text{Ti}(\text{OC}_2\text{H}_5)_4$ polymerization involves primary particles having a much broader distribution, with the result that the xerogel produced has much broader pore size distribution with pore diameters extending into the mesopore region.

Organically Modified Oxide Gels. By replacing one of the four reactive groups on a silica precursor SiX_4 with an organic group R, an organosilicon monomer RSiX_3 (R = alkyl, aryl, alkenyl), is obtained in which the organic group is attached to the silicon atom through a Si-C bond that is stable under sol-gel processing conditions. Incorporation of the organic functionality offers the opportunity to modify the physical properties of the final xerogel both directly, by organically modifying the gel, and indirectly, through the influence of the organic group on the reaction pathways followed during sol-gel processing.¹⁶⁹ In theory, hydrolysis/condensation of an organosilicon alkoxide precursor RSiX_3 as in reaction (10) should afford an organically modified



silica gel under the same reaction conditions employed to form silica from the corresponding $\text{Si}(\text{OR})_4$ precursor as in reaction (4). In practice, $(\text{RSiO}_{1.5})_n$ polyorganosilsesquioxane gels are readily obtained only from the polymerization of methyltrialkoxysilanes.¹⁷⁰ Silsesquioxane monomers with more sterically bulky substituents rarely lead to gels under conventional sol-gel processing conditions.¹⁷¹ Instead, lower molecular weight, soluble materials known as organosilsesquioxane resins are formed.^{172,173} Polysilsesquioxane gels can be prepared, however, under emulsion polymerization conditions, i.e., heterogeneous polymerization of the monomers in aqueous dispersions.^{174,175} Under these conditions, gelation rates still decrease with increasing steric bulk of the organic substituent. Interestingly, mesopore size in the xerogels increases with increasing size of the organic functionality in the order methyl, vinyl, phenyl.¹⁷⁵

Some of the difficulties associated with sol-gel polymerization of simple organosilicon precursors RSiX_3 can be circumvented by using polyfunctional precursors in which two or more triethoxysilyl groups are bonded to single arylene, alkylene, alkenylene, or acetylene bridging group as shown in Scheme 2.¹⁷⁶ In almost all cases, these monomers produce bridged polysilsesquioxane gels in minutes to hours under sol-gel processing conditions. For example, arylene-bridged gels form so readily at high monomer concentrations ($>1.8 \text{ M}$) that gelation occurs before the solution can be completely mixed. At lower monomer concentrations, 1,4-phenylene-bridged gels can be prepared in alcohols,¹⁷⁷ tetrahydrofuran,¹⁷⁷ toluene (using surfactants and phase transfer catalysts),¹⁷⁸ and even in supercritical carbon dioxide.¹⁷⁹ Longer gelation times are observed with alkylene-bridged 1,2-ethylene, 1,3-propylene and 1,4-butylene precursors that form less reactive cyclic disilsesquioxanes under acidic conditions¹⁸⁰ and with the sterically congested and unreactive 4,5-bis(triethoxysilyl)norbom-2-ene precursor.¹⁸¹

Bridged polysilsesquioxane xerogels based on rigid arylene, ethenylene, or acetylene bridging groups are high surface area, microporous materials. For example, 1,4-phenylene-bridged xerogels exhibit Type I Ar adsorption isotherms and have apparent BET surface areas approaching $1000 \text{ m}^2/\text{g}$, indicating significant microporosity.¹⁷⁷ Arylene-bridged aerogels prepared by supercritical carbon dioxide extraction retain this microporosity but in addition have significant mesoporosity, leading to apparent BET surface areas as high as $1,865 \text{ m}^2/\text{g}$.¹⁸² The surface areas and porosities of bridged polysilsesquioxane xerogels based on flexible alkylene-bridging groups are dependent upon the length of the bridging group employed. This effect has been examined in a series of alkylene-bridged gels with bridging groups ranging from ethylene- to tetradecylene- that were prepared under acidic and basic conditions and then dried both under supercritical conditions and evaporatively. The aerogels were all mesoporous materials with surface areas between $100\text{-}1,000 \text{ m}^2/\text{g}$ that exhibited significant shrinkage during drying despite the supercritical conditions.¹⁸³ In contrast, mesoporosity was observed in xerogels prepared under acidic conditions only when alkylene-bridging groups shorter than the butylene group were employed and in xerogels prepared under basic conditions only when alkylene-bridging groups

shorter than the tetradecylene group were employed.^{176a,184} In each case, longer alkylene bridging groups gave materials that were nonporous to nitrogen and, in the case of the hexylene bridging groups under acidic conditions, carbon dioxide. In addition, pore sizes determined for the base catalyzed gels exhibited a direct dependence on length of the bridging group. The porosities of bridged silsesquioxane is most simply related to the nature of the bridging group in terms of the structural rigidity of the bridging group. Presumably, rigid arylene bridging groups not only inhibit the formation of small cyclic structures but also produce relatively noncompliant networks, such that collapse of porosity is inhibited during drying. In the case of the more flexible alkylene bridging groups, collapse of porosity during drying may be due to the greater compliance of the less condensed, acid-catalyzed materials employing linear alkylene bridging groups containing more than six carbon atoms. The gels prepared using base catalysts exhibit higher degrees of condensation such that longer alkylene bridging groups are needed to make the gels compliant enough for collapse of porosity during drying.

Several strategies have been used in attempts to modify the organosilsesquioxane gels using secondary chemical processes. One successful approach involves preparing a porous or non-porous xerogel and using the organic bridging group as a pore template. By taking advantage of the differences in thermal and chemical stabilities between the siloxane and organic components of these gels it is possible to selectively liberate part or all of the organic group. This strategy has been successfully applied to organosilsesquioxane polymers by thermally oxidizing pendant organic groups to generate microporous materials.¹⁸⁵ Similarly, alkylene- and arylene-bridging groups can be selectively removed using a low temperature inductively coupled oxygen plasma to burn away the organic components and leave behind porous silica gels (Scheme 3).¹⁸⁶ When non-porous alkylene-bridged xerogels are used, the mean pore size is proportional to the length of the bridging alkylene group. Not only can porous silica gels be generated with some degree of control over porosity, but information concerning the organic domain can be obtained through characterization of the pores.

Organic bridging or pendant groups can also provide platforms for attaching functional groups that can act as metal ligands and provide additional reversible, bonding interactions with which to organize the growing polymer before gelation occurs. Several groups have used amino- and mercapto-functionalized alkyltriethoxysilanes to bind metal centers and generate siloxane gels with homogeneously dispersed metal clusters.^{187, 188} Formation of coordination complexes with a single metal or metal cluster using several precursor molecules potentially permits the self-assembly of a bridged silsesquioxane before or during the sol-gel polymerization. Complexation of metals using pendant or bridging groups containing olefinic^{188, 189} or acetylenic¹⁹⁰ functionalities is another successful strategy for changing the sol-gel chemistry. Corriu was able to show significantly faster gelation times with a 2-butenylene-bridged precursor in the presence of palladium(II) salts.¹⁸⁹ Similarly, palladium salts have been shown to decrease gel times in ethenylene-bridged systems by over three order of magnitude.¹⁹¹ This chemistry is complicated by the reduction of palladium(II) salts to palladium(0) nanoclusters driven by the oxidation of ethanol liberated during the sol-gel polymerization. However, rhodium and ruthenium salts can also be used to coordinatively reduce gelation rates for the ethenylene-bridged monomer while still in the mononuclear form.¹⁹¹

Porous Heteropolyanion Salts

Heteropolyanions are large, anionic metal oxide clusters whose salts are often porous materials.^{192, 193} Because certain heteropolyanion salts are thermally stable and chemically reactive, porous heteropolyanion salts have attracted much attention as heterogeneous catalysts.^{193, 194} The structures of heteropolyanion salts are well-defined on three levels of organization: primary, secondary, and tertiary. As shown for the phosphotungstate anion $[\text{PW}_{12}\text{O}_{40}]^{3-}$ in Figure 12, the molecular structure of a heteropolyanion defines the primary structure, and the secondary structure is defined by the arrangement of the heteropolyanions, the counterions, plus any other constituent molecules in three-dimensional space. Small crystallites of heteropolyanion salts sometimes serve as primary particles that aggregate into secondary

particles, and this arrangement defines the tertiary structure. With respect to the pore structure, the tertiary structure is important, since the polyanion framework (primary structure) is only 1-1.5 nm in size and usually nonporous. The secondary structure is as a rule also nonporous. Hence, pores are formed in the space between the primary particles of aggregates. Salts of the so-called Keggin-type heteropolyanions $[XM_{12}O_{40}]^{n-}$ and Dawson-type heteropolyanions $[X_2M_{18}O_{62}]^{n-}$ are the most thoroughly studied heteropolyanion salts and the former have found large-scale industrial application as heterogeneous catalysts.¹⁹⁵

Heteropolyanion salts are known to display two fundamentally different types of adsorption and are classified accordingly as A-class and B-class salts.¹⁹⁶ A-class salts are water-soluble compounds containing small monovalent or multivalent cations such as Na^+ , H^+ , or Ni^{2+} , and are non-porous and low surface area solids in terms of their ability to sorb nitrogen. However, these solids exhibit unique “pseudoliquid” absorption behavior toward polar molecules that plays an important role in catalysis. B-class salts contain cations such as Cs^+ , K^+ , and NH_4^+ , and are water-insoluble. These materials have high porosity in terms of surface areas derived from nitrogen gas sorption isotherms.

Pseudoliquid Phase Behavior. Large amounts of polar materials such as alcohols and amines are absorbed stepwise as a function of partial pressure into the solid bulk of A-class salts such as $H_3PW_{12}O_{40}$,¹⁹⁷ either reversibly or irreversibly, while only small amounts of non-polar materials such as hydrocarbons and N_2 are adsorbed, and these are adsorbed only on the surface of the heteropolyanion salt. This polarity- (or basicity-) selective sorption into the ionic heteropolyanion salt lattice sometimes results in expansion of the lattice dimensions. In the case of ethanol absorption by the polyacid $H_3PW_{12}O_{40}$, NMR studies have shown that both the proton and alcohol mobilities as well as the rate of proton exchange between the polyacid and absorbed alcohol increase as the number of adsorbed alcohol molecules increases.¹⁹⁸ In the case of pyridine (py) absorption by $H_3PW_{12}O_{40}$, single-crystal XRD¹⁹⁹ and infrared spectroscopic studies have shown show that stable stoichiometric crystalline salts $H_3PW_{12}O_{40} \cdot 6py$ are formed in which $py \cdots H^+ \cdots py$ groups are present.

Pore Structure of Cs and NH₄ Salts. The surface areas of H₃PW₁₂O₄₀ and its sodium salt are low and both materials show Type II nitrogen adsorption isotherms, reflecting their nonporous nature. The B-class acidic cesium salts of H₃PW₁₂O₄₀, that is, Cs_xH_{3-x}PW₁₂O₄₀ or CsX, display very different behavior.²⁰⁰ Here, surface area increases rapidly when $x > 2$ and reaches 150-170 m²g⁻¹ when $2.5 < x < 3.0$. The isotherms for $x > 2.3$ show the presence of mesopores in the region of 3-6 nm in addition to increased porosity in the micropore region. The size of these mesopores increases with increasing x , indicating that the pore size can be controlled. As a result, shape-selective adsorption and catalysis is observed for several liquid-phase reactions catalyzed by CsX.^{200,201}

The adsorption of different gas phase probe molecules by CsX has also been used to demonstrate that the size of micropores in CsX changes gradually with x .²⁰¹ As shown in Table 3, the average micropore diameter is < 0.59 nm for Cs2.1, 0.62-0.75 nm for Cs2.2, and > 0.85 nm for Cs2.5. BJH and HK analyses for meso- and micropores, respectively, are in semi-quantitative agreement with these results. Phosphorus-31 NMR spectra of CsX display four resonances which have been assigned to the polyanions associated with 0, 1, 2, and 3 protons, respectively. As the relative intensities of the four lines agree with the statistical distribution in accordance with the x value, the salts are seen to be nearly uniform solid solutions of H₃PW₁₂O₄₀ and Cs₃PW₁₂O₄₀. Particle sizes estimated from surface area by assuming spherical primary particles were comparable with those estimated from XRD linewidths only when $x > 2.2$; the first estimate greatly exceeded the second for $x = 1$ and 2.

Another interesting feature of B-class salts is the epitaxial self-assembly of primary particles leading to tertiary structure of the type shown in Figure 12. In the case of [PW₁₂O₄₀]³⁻ precipitated as an ammonium salt or as a cesium salt at elevated temperatures, dodecahedra having similar size have been observed by SEM to be composed of primary particles 10 to 20 nm in size (see Figure 13).²⁰² The BET surface areas measured for these materials were much greater than those estimated from the dodecahedra observed by SEM, showing that the dodecahedra are porous and the particles seen by SEM are secondary particles. However, the particle size estimated from the

XRD line width was close to that observed in the SEM photographs and much greater than those calculated using BET theory. This is in contrast to CsX case, $x > 2.2$, described above, indicating that the crystal planes of the primary particles (crystallites) observed by SEM are aligned, making the secondary particles more or less like a porous single crystal. Electron diffraction patterns were in agreement with this idea. A possible explanation for the formation of an epitaxial interface between primary particles is that reorientation of the microcrystalline primary particles, accompanied by slight dissolution at the outer surface, can take place during the assembly of preformed microcrystallites. In this case, solubility is the key factor controlling the self-assembly process.

Research Needs and Opportunities

The tailoring of porous materials poses a broad challenge that is perhaps best appreciated by considering the range of applications where specific types of new porous materials are needed for use in devices or systems that perform specific functions. Examples include shape-selective gas or liquid permselective membranes, catalytic membrane reactors, energy storage systems such as batteries, and on a longer time scale, molecular electronic and electrooptic devices as well as biomolecule separation, isolation, and delivery. These applications will require tailoring not only on the molecular size scale, the domain of chemical synthesis, but also on the meso- and macroscopic size scale, the domain of materials processing. For example, porous carbons are difficult to tailor on the molecular size scale, but they can be processed into the specific geometries required for different applications. In contrast, oxide molecular sieves with specific pore sizes and shapes are available for specific applications, but they are easily obtained only as micron-sized crystals. As a result, molecular sieve catalysts are frequently used as supported systems, usually on amorphous oxides. In these cases it would be desirable to tailor the self-assembly of microcrystalline sieve materials into agglomerates. For the fabrication of truly shape-selective membranes, molecular sieve materials should ideally be available as very thin (0.1 to 10 μm) films

over surface areas of one to several square meters where micro- or mesopores are all aligned in the direction of the permeating flow.

Many scientific and technological problems must be addressed before porous materials can be tailored to the same extent possible with other important classes of engineering materials such as semiconductors, dielectric ceramics, organic polymers, and metallic alloys. Historically, these problems have been addressed by focusing on specific types of materials such as molecular sieves or porous carbons or specific applications such as gas separation or catalysis rather than investigating the fundamental scientific issues involved. Research opportunities addressing these issues are the focus of attention in this section, since resolution of fundamental scientific issues will impact a broad range of materials and applications.

Perhaps the most fundamental issue involved in tailoring porous materials is the nature of adsorbent-adsorbate interactions and the relationship between these interactions and sorption kinetics and thermodynamics. The nature of relatively "simple" adsorbent-adsorbate interactions involving electrostatic forces in heteroatom substituted zeolites is not well understood, and far more complex interactions must be considered in coordination solids that show chemical selectivity for specific types of molecules such as aromatics or specific molecules such as oxygen. The use of effective intermolecular potentials remains an important aspect of molecular modeling, and a careful assessment of the accuracy of such approaches along the lines of Pellenq and Nicholson²⁰³ should prove to be useful starting point. Improvements in quantum mechanical methods also offer promise in this area as do the development of new experimental techniques which directly probe adsorbent-adsorbate interactions. New molecular simulation techniques and new statistical mechanical theories are also emerging that allow for improved modeling of sorption kinetics and thermodynamics. Further development and application of nonequilibrium molecular dynamics techniques^{41,42} offer the prospect of better understanding transport processes known to be important in kinetics based adsorption separations.³⁷ This prospect is particularly relevant to multicomponent adsorption and surface diffusion in carbon molecular sieve membrane separations where the influence of pressure, temperature, and pore structure on selectivity is poorly understood

and therefore difficult to control. Future progress in statistical mechanical theories such as density functional theory should lead to a better understanding of the behavior of complex adsorbates such as chain molecules²⁶ as well as adsorbents having complex pore geometries²⁷ and disordered structures.^{204,205} Further developments in molecular modeling techniques for adsorbents that behave as deformable solids^{13,14} or even undergo adsorbate-induced phase transitions^{29,30,32,33} should also be anticipated.

Zeolites, mesoporous molecular sieves, and sol-gel derived oxides are all prepared from oxide gels, and advances in the processing of these materials will require a better physical understanding of how porosity evolves in gels and in porous materials that crystallize from gels. Most notably, the mechanism of nucleation and growth of ordered domains in gels has not been adequately explored. The challenge here is to develop effective *in situ* techniques that will allow systematic studies of local ordering and nucleation rates as a function of synthesis and processing conditions. There is a particular need to study the detailed role of templating agents, especially in nonsilicious systems. During sol-gel processing, the mechanical properties of a gel can also influence the evolution of its pore structure and these mechanical properties are controlled by the gel's network structure. No methods are currently available, however, for measuring the connectivity of the network. Improved modeling and measurement techniques are also needed to understand the rigidity of gel networks. Several models exist that explain the power-law dependence of the modulus on the density, but they have not yet been adequately tested by obtaining data on the structure and the mechanical properties of the same samples. Improved models are needed to explore the mechanism of pore formation in such cases. These considerations are particularly important for the development of size-selective membranes.

In order to design and construct porous materials with well defined porosities on the molecular size scale in noncrystalline materials, the general question of how porosity can be controlled through polymerization of well-defined molecular building units requires further investigation. In general, the structural evolution of the inorganic polymers on the molecular level needs to be studied beyond the oligomeric stages that are easily probed spectroscopically, possibly

using mass spectrometry, chromatography, scattering techniques and high field nuclear magnetic resonance techniques. Continued efforts to use new chemistry to preorganize monomers reversibly before crosslinking takes place may bring a higher degree of control over porosity in these materials and possibly provide improved mechanical properties by allowing the reversible bonds to rearrange and permit maximum connectivity to be achieved in the ultimate product. It may be possible in this fashion to achieve the goal of preparing tailored materials that are sufficiently ordered over short distances to serve as selective adsorbents but sufficiently disordered over long distances to avoid crystallization and thus remain processible.

Tremendous advances have been made in tailoring the porosity of oxide molecular sieves and porous carbons in terms of size and shape selectivity. Relatively little progress has been achieved, however, in terms of chemoselectivity, that is, selectivity for specific molecules or functional groups based on their chemical reactivity as opposed to their physical size or shape. The incorporation of active sites into these materials is therefore a high priority. Other classes of materials such as porous coordination solids, sol-gel derived oxides, and porous heteropolyanion salts offer great promise in this regard since they can be prepared from well-defined molecular precursors containing a variety of metal and nonmetal centers under relatively mild conditions. To date, impressive results have been obtained with porous coordination solids by using π - π stacking interactions to achieve selective binding of aromatic hydrocarbons^{96c} and metal ligand interactions to achieve selective binding of oxygen molecules^{105,106,107} and organic alcohols¹⁰⁸. There is tremendous potential for expanding this type of chemoselectivity where coordinatively unsaturated metal centers, hydrogen bond acceptors, hydrogen bond donors, or virtually any type of active sites are incorporated into the framework of a porous material: incoming guest molecules must not only have the appropriate shape and size but also the required affinity for the active sites present. Analogous materials with charged frameworks capable of reversible ion exchange also offer opportunities for achieving chemoselectivity by tailoring cation or anion binding sites to create an affinity for specific anions or cations.

Given the wide variety of porous materials that are currently available, it is hardly surprising that most current research devoted to tailoring porous materials is concerned with development of known routes to porous materials rather than exploration of entirely new approaches. Nonetheless, there is a pressing need to reach beyond the traditional techniques generally associated with the synthesis and processing of porous materials, that is, hydrothermal treatment, gel crystallization, coordination polymerization, gelation, pyrolysis, and precipitation. Exploration of entirely new approaches to the preparation porous materials promise to open up new research opportunities for tailoring porous materials, both new materials and old materials.

Acknowledgments. This panel study was sponsored by the Council on Materials Research of the United States Department of Energy, Office of Basic Energy Sciences, Division of Materials Sciences.

Sandia is a multiprogram laboratory operated by Sandia Corporation, a Lockheed Martin Company, for the United States Department of Energy under contract DE-AC04-94AL85000.

Figure Captions

Figure 1. IUPAC classification of adsorption isotherms.

Figure 2. Types of adsorption isotherms obtained from slit pore model using density functional theory. The three large diagrams shown on the left qualitatively indicate which types of adsorption isotherms are obtained as a function of fluid-solid interaction strength $\epsilon_{sf}/\epsilon_{ff}$ and pore wall separation H^* at three different temperatures, $T^* = 0.5, 0.8,$ and 1.4 , corresponding to low temperature, intermediate temperature, and supercritical regimes. The actual isotherms are shown on the right, labeled according to the IUPAC classification shown in Figure 1. (Reprinted with permission from ref 23. Copyright 1993 American Chemical Society.)

Figure 3. The formation of microporous molecular sieves using individual small alkyl chain length quaternary directing agents (top). The formation of mesoporous molecular sieves using long alkyl chain length quaternary directing agents (bottom).

Figure 4. The X-ray diffraction patterns and proposed structures of MCM-41, MCM-48, and MCM-50.

Figure 5. Transmission electron micrographs of MCM-41 materials having pore sizes of 20, 40, 65, and 100 Å. (Reprinted with permission from ref 59. Copyright 1992 American Chemical Society.)

Figure 6. The crystal structure of $\text{Ag}(4,4'\text{-bpy})\text{NO}_3$ viewed along the crystallographic [100] direction. Only one of the three interpenetrating $\text{Ag}(\text{bpy})^+$ frameworks is shown in a ball-and-stick representation with silver atoms drawn as filled spheres, carbon atoms as open spheres, and nitrogen atoms as shaded spheres. The large shaded spheres represent the oxygen atoms of the nitrate ions.

Figure 7. A perspective drawing of the solid state structure of $\text{Co}[\text{C}_6\text{H}_3(\text{COOH}_{1/3})_3](\text{NC}_5\text{H}_5)_2 \cdot 2/3\text{NC}_5\text{H}_5$ perpendicular to the crystallographic z-axis. The $\text{Co}[\text{C}_6\text{H}_3(\text{COOH}_{1/3})_3](\text{NC}_5\text{H}_5)_2$ layers are shown as ball and stick models, and the intercalated pyridine guest molecules are shown as space-filling models. Cobalt atoms are represented by filled

spheres, carbon atoms by shaded spheres, nitrogen atoms by partially shaded spheres, and oxygen atoms by unshaded, open spheres.

Figure 8. Transient adsorption of pure O₂ and N₂ by a CMS. (Reprinted with permission from ref 119. Copyright 1995 Elsevier Science Ltd.)

Figure 9. Adsorption and diffusion through CMS membrane pores. (Reprinted with permission from ref 119. Copyright 1995 Elsevier Science Ltd.)

Figure 10. Capillary gas chromatogram of Si(OCH₃)₄ hydrolysis products showing assignments of molecular formulas and structures. Structural diagrams represent the [Si_xO_y] core structures of [Si_xO_y](OCH₃)_z molecules using dots to represent silicon atoms and lines to represent oxygen atoms linking these centers. (Reprinted with permission from ref 163. Copyright 1988 Materials Research Society.)

Figure 11. Transmission electron micrographs of platinum replicated (a) [Si₈O₁₂](OCH₃)₈-derived and (b) Si(OCH₃)₄-derived xerogels.

Figure 12. Primary, secondary, and tertiary structures of heteropolyanion compounds. (Reprinted with permission from ref 193. Copyright 1996 Academic Press, Inc.)

Figure 13. Scanning electron micrograph of (NH₄)₃PW₁₂O₄₀ precipitated at 368° K.

Table 1. Pore volumes (cm^3g^{-1}) for coal-based active carbons.¹¹⁴


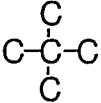
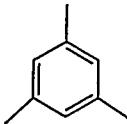
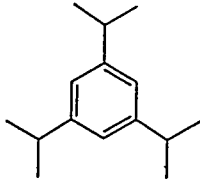
Coal Precursor	Micropores	Mesopores	Macropores
Anthracite	0.51	0.07	0.11
Bituminous	0.43	0.17	0.26
Lignite	0.22	0.58	0.32
Blended	0.42	0.11	0.33

Table 2. Permeabilities of components of a hydrocarbon(HC)-hydrogen gas mixture^a through a CMS membrane at 295.1 K.¹¹⁹

Gas	Permeability (Barrer)	Selectivity over H ₂ from mixture (P_{HC}/P_{H_2})	Permeability ratio pure gases ($P_{HC}^{\circ}/P_{H_2}^{\circ}$)
H ₂	1.2	1.0	1.0
CH ₄	1.3	1.1	5.1
C ₂ H ₆	7.2	6.0	6.6
C ₃ H ₈	24.1	20.1	2.2
C ₄ H ₁₀	120.0	100.0	1.2

^a 41.0% H₂, 20.2% CH₄, 9.5% C₂H₆, 9.4% C₃H₈, 19.9% C₄H₁₀

Table 3. Sorptive properties of CsX, X = 2.1, 2.2 and 2.5.²⁰¹

Molecule	Kinetic Diameter /Å	Amount/ $\mu\text{mol g}^{-1}$			Ratio to Cs2.5	
		Cs2.1	Cs2.2	Cs2.5	Cs2.1	Cs2.2
N ₂	3.6	487	861	1648	0.30	0.52
	5.9	10	124	232	0.04	0.53
	6.2	5	179	390	0.01	0.46
	7.5	-	11	237	-	0.05
	8.5	-	15	236	-	0.06

References

- (1) Gregg, S. J.; Sing, K. S. W. *Adsorption, Surface Area and Porosity*, 2nd ed.; Academic: London, 1982.
- (2) Spinoza, B. *Ethics*; Everyman's Library, No. 481; J. M. Dent & Sons: London, 1941; p 14.
- (3) Nicholson, D.; Parsonage, N. G. *Computer Simulation and the Statistical Mechanics of Adsorption*; Academic: London, 1982.
- (4) Langmuir, I. *J. Am. Chem. Soc.* 1913, 35, 931; 1915, 37, 1139; 1918, 40, 1361.
- (5) Brunauer, S. *The Adsorption of Gases and Vapors*; Princeton University: Princeton, 1943.
- (6) Sing, K. S. W.; Everett, D. H.; Haul, R. A. W.; Moscou, L.; Pierotti, R. A.; Rouquérol, J.; Siemieniewska, T. *Pure & Appl. Chem.* 1985, 57, 603.
- (7) McEnaney, B.; Mays, T. J. In *Porosity in Carbons*; Patrick, J. W., Ed.; E. Arnold: London, 1995; p 93.
- (8) Guinier, A.; Fournet, G. *Small Angle Scattering of X-rays*; Wiley: New York, 1955.
- (9) Brun, M.; Lallemand, A.; Quinson, J. F.; Eyraud, C. *Thermochim. Acta.* 1977, 21, 59.
- (10) (a) Liu, H.; Zhang, L.; Seaton, N. A. *Chem. Eng. Sci.* 1992, 47, 4393. (b) Reference 1, pp 150 - 152. (c) Scherer, G. W. submitted for publication.
- (11) Reference 1, pp 228 - 233.
- (12) Lowell, S.; Shields, J. E. *Powder Surface Area and Porosity*, 3rd ed.; Chapman and Hall: New York, 1991; p 59.
- (13) Nicolaon, G. A.; Teichner, S. J. *Bull. Soc. Chim. Fr.* 1968, 9, 3555.
- (14) Scherer, G. W.; Smith, D. M.; Stein, D. J. *Non Cryst. Solids* 1985, 186, 309.
- (15) Scherer, G. W.; Alviso, C.; Pekala, R.; Gross, J. In *Microporous and Macroporous Materials*; Lobo, R. F., Beck, J. S., Suib, S. L., Corbin, D. R., Davis, M. E., Iton, L.

- E.; Zones, S. I. Eds.; MRS Symp. Proc.; Materials Research Society: Pittsburgh, PA, 1996; Vol. 431, p 497.
- (16) Reference 1, pp 233- 239.
- (17) Cracknell, R. F.; Gubbins, K. E.; Maddox, M.; Nicholson, D. *Accts. Chem. Res.* 1995, 28, 281.
- (18) Steele, W. A., *The Interactions of Gases with Solid Surfaces*; Pergamon: Oxford, 1973.
- (19) (a) MacElroy, J. M. D.; Raghavan, K. *J. Chem. Phys.* 1990, 93, 2068. (b) Kaminsky, R. D.; Monson, P. A. *J. Chem. Phys.* 1991, 95, 2936.
- (20) Maitland, G. C.; Rigby, M.; Smith, E. B.; Wakeham, W. A. *Intermolecular Forces: Their Origin and Determination*; Clarendon: Oxford, 1981.
- (21) (a) Evans, R. In *Fundamentals of Inhomogeneous Fluids*; Henderson, D., Ed.; Dekker: New York, 1992. (b) Evans, R. *J. Phys.: Condens. Matter*, 1990 2, 8989 .
- (22) (a) Lastoskie, C.; Gubbins, K. E.; Quirke, N. *Langmuir* 1993, 9, 2693. (b) Seaton, N. A.; Walton, J.P.R.B.; Quirke, N. *Carbon* 1989, 27, 853. (c) Lastoski, C.; Gubbins, K. E.; Quirke, N. *J. Phys. Chem.* 1993, 97, 4789. (d) Olivier, J. P.; Conklin, W. B.; von Szombatheley, M. In *Characterization of Porous Solids III*; Rouquerol, J., Rodriguez-Reinoso, F., Sing, K. S. W., Unger, K. K. Eds.; Studies in Surface Science and Catalysis 87; Elsevier: Amsterdam, 1994; p 81. (e) Vanslooten, R.; Bojan, M. J.; Steele, W. A. *Langmuir* 1994, 10, 542. (f) Bojan, M. J.; Vernov, A. V.; Steele, W. A. *Langmuir* 1992, 8, 901. (g) Mays, T. J.; Seaton, N. A.; McEnaney, B. *Proc. International Conference Carbon '94*, 1994, 656. (h) Mays, T. J. In *Fundamentals of Adsorption*; LeVan, M. D., Ed.; Kluwer: Amsterdam, 1996; p. 603.
- (23) Balbuena, P. B.; Gubbins, K. E. *Langmuir* 1993, 9, 1801.
- (24) See, for example: (a) Kierlik, E.; Rosinberg, M. L. *Phys. Rev. A* 1991, 44, 5025. (b) Tan, Z.; Gubbins, K. E. *J. Phys. Chem.* 1992, 96, 845. (c) Kierlik, E.; Rosinberg, M.

- L.; Finn, J. E.; Monson, P. A. *Molec. Phys.* 1992, 75, 1435. (d) Sowers, S. L., Gubbins, K. E. *Langmuir* 1995, 11, 4758.
- (25) Kierlik, E.; Fan, Y.; Monson, P. A.; Rosinberg, M. L. *J. Chem. Phys.* 1995, 102, 3712.
- (26) M.Kierlik, E.; Rosinberg, M. L. *J. Chem. Phys.* 1994, 100, 21716.
- (27) Mitchell, M. C.; McCormick, A. V.; Davis, H. T. *Z. Phys. B* 1995, 97, 353.
- (28) Allen, M. P.; Tildesley, D. J. *Computer Simulation of Liquids*; Clarendon Press; Oxford: 1987.
- (29) Pellenq, R. J-M.; Nicholson, D. *Langmuir* 1995, 11, 1626.
- (30) Snurr, R. Q.; Bell, A. T.; Theodorou, D. N. *J. Phys. Chem.* 1993, 97, 13742.
- (31) (a) Cracknell, R. F.; Gubbins, K. E., *Langmuir* 1993, 9, 824. (b) Cracknell, R. F.; Gubbins, K. E. In *Fundamentals of Adsorption*; Suzuki, M. Ed.; Studies in Surface Science and Catalysis 80; Elsevier: Amsterdam, 1993; p 105.
- (32) Llewellyn, P. L.; Coulomb, J-P.; Grillet, Y.; Patarin, J.; Lauter, H.; Reichert, H.; Rouquerol, J. *Langmuir* 1993, 19, 1846.
- (33) Tosi-Pellenq, N. M.; Coulomb, J-P., 1993, unpublished data cited in reference 17.
- (34) (a) Karavias, F.; Myers, A. L. *Molec. Simulation* 1991, 8, 51. (b) Razmus; D. M.; Hall, C. K. *AICHE. J.* 1991, 37, 5. (c) Maddox, M. W.; Rowlinson, J. S. *J. Chem. Soc. Faraday* 1993, 89, 3619. (d) Van Tassel, P. R.; Davis, H. T.; McCormick, A. V. *Langmuir* 1994, 10, 1257. (e) Somers, S. A.; McCormick, A. V.; Davis, H. T. *J. Chem. Phys.* 1993, 99, 9890. (f) Cracknell, R. F.; Nicholson, D.; Quirke, N. *Mol. Phys.* 1993, 80, 885. (g) Peterson, B. K.; Heffelfinger, G. S.; Gubbins, K. E.; van Swol, F. *J. Chem. Phys.* 1990, 93, 679.
- (35) Kaminsky, R. D. *J. Chem. Phys.* 1994, 101, 4986.
- (36) Frenkel, D.; Smit, B. *Understanding Molecular Simulation*; Academic Press: San Diego, 1996.

- (37) Ruthven, D. M. *Principles of Adsorption and Adsorption Processes*; John Wiley: New York, 1984.
- (38) June, R. L.; Bell, A. T.; Theodorou, D. N. *J. Phys. Chem.* 1990, *94*, 8232.
- (39) Caro, J.; Bulow, M.; Schirmer, W.; Karger, J.; Heink, W.; Pfeifer, H.; Zdanov, S. *J. Chem. Soc., Faraday Trans.* 1985, *81*, 2541.
- (40) Jobic, H.; Bee, M.; Karger, J. In *Zeolites for the Nineties, Recent Research Reports*; Jansen, J. C., Moscou, L., Post, M. F. M. Eds.; Presented at the International Zeolite Conference, Amsterdam, The Netherlands, June 1989; p 305.
- (41) Maginn, E. J.; Bell, A. T.; Theodorou, D. N. *J. Phys. Chem.* 1993, *97*, 4173.
- (42) (a) Heffelfinger, G. S.; van Swol, F. *J. Chem. Phys.* 1994, *100*, 7548. (b) MacElroy, J. M. D. *J. Chem. Phys.* 1994, *101*, 5274. (c) Cracknell, R. F.; Nicholson, D.; Quirke, N. *Phys. Rev. Letters* 1995, *74*, 2463.
- (43) Dyer, A. *An Introduction to Zeolite Molecular Sieves*; Wiley: Chichester, 1988.
- (44) McBain, J. *The Sorption of Gases and Vapours by Solids*; George Routledge & Sons, Ltd: London, 1932; p 167.
- (45) Chen, N.; Degnan, T.; Smith, C. *Molecular Transport and Reaction in Zeolites*; VCH: New York, 1994; p 223.
- (46) Plank, C. *Heterogeneous Catalysis: Selected American Histories*; American Chemical Society: Washington, DC, 1983; p 253.
- (47) Venuto, P. *Microporous Materials* 1994, *2*, 297.
- (48) (a) Armor, J. In *Materials Chemistry: An Emerging Discipline*; Caspar, L., Ellis, A., Interrante, L. Eds.; Advances in Chemistry Series 245, American Chemical Society: Washington, DC, 1995; p 321. (b) Masuda, T; Tsutsumi, K; Takahashi, H. *Journal of Colloid and Interface Science* 1980, *77*, 238. (c) Gaffney, T. *Current Opinion in Solid State and Materials Science* 1996, *1*, 69. (d) Razmus, D.; Hall, C. *AIChE Journal* 1991, *37*, 769.

- (49) Kleinschmidt, P. In *Industrial Inorganic Chemicals: Production and Uses*; Thompson, R., Ed.; The Royal Society of Chemistry: London, 1995; p 344.
- (50) *Intercalation Chemistry*; Whittingham, H. S., Jacobson, A. S. Eds.; Academic Press: New York, 1982.
- (51) Nicoud, J. P. *Science* **1994**, *263*, 636.
- (52) Landis, M. E.; Aufdembrink, B. A.; Chu, P.; Johnson, I. D.; Kirker, G. W.; Rubin, M. K. *J. Am. Chem. Soc.* **1991**, *113*, 3189.
- (53) Pinnavaia, T. J. *Science* **1983**, *220*, 365.
- (54) Lagaly, G.; Beneke, K. *Colloid. Polm. Sci.* **1991**, *269*, 1198.
- (55) *Pillared Layered Structures: Current Trends and Applications*; Mitchell, I. V., Ed.; Elsevier Science: Amsterdam, 1990.
- (56) *Synthesis of Microporous Materials*; Ocelli, M. L., Robson, H. Eds; Van Nostrand: New York, 1992; Vol. II.
- (57) *Introduction to Zeolite Science and Practice*; Van Bekkum, H., Flanigen, E. M., Jansen, J. C., Eds.; Studies in Surface Science and Catalysis 58; Elsevier: Amsterdam, 1991.
- (58) Kresge, C. T.; Leonowicz, M. E.; Roth, W. J.; Vartuli, J. C.; Beck, J. S. *Nature* **1992**, *359*, 710.
- (59) Beck, J. S.; Vartuli, J. C.; Roth, W. J.; Leonowicz, M. E.; Kresge, C. T.; Schmitt, K. D.; Chu, C. T.-W.; Olson, D. H.; Sheppard, E. W.; McCullen, S. B.; Higgins, J. B.; Schlenker, J. L. *J. Am. Chem. Soc.* **1992**, *114*, 10834.
- (60) Barrer, R. M. *Hydrothermal Chemistry of Zeolites*; Academic Press: London, 1982.
- (61) (a) Davis, M. E. In *Zeolites: A Refined Tool for Designing Catalytic Sites*; Bonneviot, L., Kaliaguine, S. Eds.; Studies in Surface Science and Catalysis 97; Elsevier: Amsterdam, 1995; p 35. (b) Lobo, R. F.; Zones, S. I.; Davis, M. E. *J. Inclusion Phen. Mol. Recognition in Chem* **1995**, *21*, 47.
- (62) Reference 60, pp 174 - 175 and 186 - 246.

- (63) Petrovic, I.; Natvrotsky, A.; Zones, S. I.; Davis, M. E. *Chem. Mater.* **1993**, *5*, 1805.
- (64) Henson, N. J.; Cheetham, A. K.; Gale, J. D. *Chem. Mater.* **1994**, *6*, 1647.
- (65) Reference 60, pp 151 - 174.
- (66) Gies, H.; Marler, B. *Zeolites* **1992**, *12*, 42.
- (67) Gies, H. In *Inclusion Compounds*, Atwood, J.; Davies, J.; MacNicol, D. Eds.; Oxford: New York, 1991; Vol. 5, p 1.
- (68) Zones, S.I.; Olmstead, M. M.; Santilli, D. S. *J. Am. Chem. Soc.* **1992**, *114*, 4195.
- (69) Burkett, S. L.; Davis, M. E. In *Comprehensive Supramolecular Chemistry*; Atwood, J. L.; Davies, J. E. D.; MacNicol, D. D., Vogtle, F. Eds.; Pergamon: New York, 1996; Vol. 7, Chapter 16.
- (70) Lobo, R. F.; Pan, M.; Chan I.; Medrud, R.C.; Zones, S.I.; Crozier, P.A.; Davis, M. E. *J. Phys. Chem.* **1994**, *98*, 12040.
- (71) The MCM designator is Mobil Oil Corporation's nomenclature for defining novel materials. MCM is defined as Mobil Composition of Matter and the associated number is simply added chronologically based on the date of discovery. For example, MCM-36 was discovered prior to MCM-37 and is unique to all other MCM-named materials.
- (72) Kresge, C. T.; Roth, W. J.; Simmons, K. G.; Vartuli, J. C. U.S. Patent 5 229 341, 1993; assigned to Mobil Oil Corporation.
- (73) Roth, W. J.; Kresge, C. T.; Vartuli, J. C.; Leonowicz, M. E.; Fung, A. S.; McCullen, S. B. In *Catalysis by Microporous Materials*; Beyer, H. K., Karge, H. G., Kiricsi, I., Nage, J. B. Eds.; Studies in Surface Science and Catalysis 94; Elsevier Science: Amsterdam, 1995; p 801.
- (74) Schreyeck, L.; Caullet, P.; Mouganel, J. C.; Guth, J. L.; Marler, B., *J. Chem. Soc., Chem. Commun.* **1995**, 2187.

- (75) Monnier, A.; Schüth, F.; Huo, Q.; Kumar, D.; Margolese, D.; Maxwell, R. S.; Stucky, G. D.; Krishnamurthy, M.; Petroff, P.; Firouzi, A.; Janicke, M.; Chmelka, B. F. *Science* 1993, 261, 1299.
- (76) Huo, Q.; Margolese, D.; Ciesia, U.; Feng, P.; Gier, T. E.; Sieger, P.; Leon, R.; Petroff, P. M.; Schüth, F.; Stucky, G. D. *Nature* 1994, 368, 317.
- (77) Tanev, P. T.; Pinnavaia, T. J., *Science* 1995, 267, 865.
- (78) Bagshaw, S.; Prouzet, E.; Pinnavaia, T. J. *Science* 1995, 269, 1242.
- (79) Karra, V. R.; Moudrakovski, I. L.; Sayari, A. *J. Porous Mater.* 1996, 3, 77.
- (80) Beck, J. S.; Vartuli, J. C.; Kennedy, G. J.; Kresge, C. T.; Roth, W. J.; Schramm, S. E. *Chem. Mater.* 1994, 6(10), 1816.
- (81) Stucky, G. D.; Monnier, A.; Schüth, F.; Huo, Q.; Margolese, D.; Kumar, D.; Krishnamurthy, M.; Petroff, P. M.; Firouzi, A.; Janicke, M.; Chmelka, B. F. *Mol. Cryst. Liq. Cryst.* 1994, 240, 187.
- (82) Firouzi, A.; Kumar, D.; Bull, L. M.; Besler, T.; Sieger, P.; Huo, Q.; Walker, S. A.; Zasadzinski, J. A.; Glinka, C.; Nicol, J.; Margolese, D.; Stucky, G. D.; Chmelka, B. F. *Science* 1995, 267, 1138.
- (83) Huo, Q.; Margolese, D. I.; Ciesia, U.; Demuth, D. G.; Feng, P.; Gier, T. E.; Sieger, P.; Firouzi, A.; Chmelka, B. F.; Schüth, F.; Stucky, G. D. *Chem. Mater.* 1994, 6, 1176.
- (84) Chen, C.-Y.; Burkett, S. L.; Li, H.-X.; Davis, M. E. *Micro. Mater.* 1993, 2, 27.
- (85) Husson, F.; Mustacchi, H.; Luzzatti, V. *Acta Cryst.* 1960, 13, 668.
- (86) Mariani, P.; Luzzati, V.; Delacroix, H. *J. Mol. Biol.* 1988, 204, 165.
- (87) Huo, Q.; Leon, R.; Petroff, P.; Stucky, G. D. *Science* 1995, 268, 1324.
- (88) Stein, A.; Fendorf, M.; Jarvie, T. P.; Mueller, K. T.; Benesi, A. J.; Mallouk, T. E. *Chem. Mater.* 1995, 7, 304.
- (89) Luca, V.; MacLauchlan, D. J.; Hook, J. M. Withers, R. *Chem. Mater.* 1995, 7, 2220.
- (90) Abe, T.; Taguchi, A.; Iwamoto, M. *Chem. Mater.* 1995, 7, 1429.

- (91) Antonelli, D. M.; Ying, J. Y. *Angew. Chem. Int. Ed. Engl.* 1995, 34, 204.
- (92) Schüth, F. *Ber. Bunsen Ges. Phys. Chem.* 1995, 99, 1306.
- (93) Huber, C.; Moller, K.; Bein, T. *J. Chem. Soc., Chem. Commun.* 1994, 2619.
- (94) (a) Venkataraman, D.; Lee, S.; Moore, J. S.; Zhang, P.; Hirsch, K. A.; Gardner, G. B.; Covey, A. C.; Prentice, C. L. *Chem. Mater.* 1996, 8, 2030. (b) Yaghi, O. M. in *Access in Nanoporous Materials*; Pinnavaia, T. J., Thorpe, M. F. Eds.; Plenum: New York, 1995; p. 111. (c) Stein, A.; Keller, S. W.; Mallouk, T. E. *Science* 1993, 259, 1558. (d) Fagan, P. J.; Ward, M. D. *Sci. Am.* 1992, 267, 48. (e) *Supramolecular Architecture: Synthetic Control in Thin Films and Solids*; Bein, T., Ed.; ACS Symposium Series 499; American Chemical Society: Washington, DC, 1992. (f) Iwamoto, T. In *Inclusion Compounds*; Atwood, J. L., Davies, J. E. D., MacNicol, D. D. Eds.; Oxford: New York, 1991; Vol. 5, p 177.
- (95) (a) MacGillivray, L. R.; Subramanian, S.; Zaworotko, M. J. *J. Chem. Soc., Chem. Commun.* 1994, 1325-1326. (b) Yaghi, O. M.; Richardson, D. A.; Li, G.; Davis, C.; Groy T. L. In *Advances in Porous Materials*; Komarneni, S., Smith, D. M., Beck, J. S. Eds.; MRS Symp. Proc.; Materials Research Society: Pittsburgh, PA, 1995; Vol. 371, p 15. (c) Yaghi, O. M. In *Modular Chemistry*; Michl, J., Ed.; NATO ASI Series, Series C, vol. 499; Kluwer: Boston, 1997; p 663.
- (96) For example: (a) Yaghi, O. M.; Li, H.; Groy, T. L. *J. Am. Chem. Soc.* 1996, 118, 9096. (b) Robinson, F.; Zaworotko, M. J. *J. Chem. Soc., Chem. Commun.* 1995, 23, 2413. (c) Yaghi, O. M.; Li, G.; Li, H. *Nature* 1995, 378, 703. (d) Yaghi, O. M.; Li, H. *J. Am. Chem. Soc.* 1995, 117, 10401. (e) Gardner, G. B.; Venkataraman, D.; Moore, J. S.; Lee, S. *Nature* 1995, 374, 792. (f) Subramanian, S.; Zaworotko, M. J. *Angew. Chem. Int. Ed. Engl.* 1995, 34, 2127. (g) Fujita, M.; Kwon, Y. J.; Sasaki, O.; Yamaguchi, K.; Ogura, K. *J. Am. Chem. Soc.* 1995, 117, 7287. (h) Lu, J.; Harrison, W. T. A.; Jacobson, A. J. *Angew. Chem. Int. Ed. Engl.* 1995, 34, 2557. (i) Farrell, R. P.;

- Hambley, T. W.; Lay, P. A. *Inorg. Chem.* **1995**, *34*, 757. (j) Batten, S. R.; Hoskins, B. F.; Robson, R. *J. Am. Chem. Soc.* **1995**, *117*, 5385. (k) Schwarz, P.; Siebel, E.; Fischer, R. D.; Apperley, D. C.; Davies, N. A.; Harris, R. K. *Angew. Chem. Int. Ed. Engl.* **1995**, *34*, 1197. (l) Kitazawa, T.; Sugisawa, S.; Takeda, M.; Iwamoto, T. *J. Chem. Soc., Chem. Commun.* **1993**, 1855.
- (97) Ludi, A.; Gudel, H. *Struct. Bonding.* **1973**, *14*, 1.
- (98) Dunbar, K. R.; Heintz, R. A. *Prog. Inorg. Chem.* **1997**, *45*, 283.
- (99) Swanson, B. *Inorg. Chem.* **1976**, *15*, 253.
- (100) (a) Seifer, G. *Russ. J. Inorg. Chem.* **1959**, *4*, 841; **1962**, *7*, 841; **1962**, *7*, 899. (b) Boxhoorn, G.; Moolhuysen, J.; Coolegem, J. G. F.; van Santen, R. A. *J. Chem. Soc., Chem. Commun.* **1985**, 1305.
- (101) Cartraud, P.; Caintot, A.; Renaud, A. *J. Chem. Soc., Faraday Trans. 1*, **1981**, *77*, 1561.
- (102) Yaghi, O. M.; Li, H. *J. Am. Chem. Soc.* **1996**, *118*, 295.
- (103) Hoskins, B. F.; Robson, R. *J. Am. Chem. Soc.* **1990**, *112*, 1546.
- (104) Abrahams, B. F.; Hoskins, B. F.; Michail, D. M.; Robson, R. *Nature* **1994**, *369*, 727.
- (105) Ramprasad, D.; Pez, G. P.; Toby, B. H.; Markley, T. J.; Pearlstein, R. M. *J. Am. Chem. Soc.* **1995**, *117*, 10694.
- (106) Ramprasad, D.; Markley, T.; Pez, G. *J. Molecular Catalysis A* **1997**, *117*, 273.
- (107) Meier, I. K.; Pearlstein, R. M.; Panprasad, D.; Pez, G. P. *Inorg. Chem.* **1997**, *36*, 1707.
- (108) Yaghi, O. M.; Davis, C. E.; Li, G.; Li, H. *J. Am. Chem. Soc.* **1997**, *119*, 2861.
- (109) McEnaney, B.; Rand, B. *Brit. Ceram. Trans.* **1985**, *84*, 157.
- (110) Rodriguez-Reinoso, F.; Linares-Solano, A. *Physics and Chemistry of Carbon*; Thrower, P.A. Ed.; M. Dekker: New York, 1988; Vol. 21, p 1.
- (111) Jagtoyen, M.; Thwaites, M.; Stencel, J.; McEnaney, B.; Derbyshire, F. J. *Carbon* **1992**, *30*, 1089.
- (112) Jagtoyen, M.; Derbyshire, F. J. *Carbon* **1993**, *31*, 1185.

- (113) Solum, M. S.; Pugmire, R. J.; Jagtoyen, M.; Derbyshire, F. J. *Carbon* 1995, 33, 1247.
- (114) Wilson, J. *Fuel* 1981, 60, 823.
- (115) Oberlin, A.; Villey, M.; Combaz, A. *Carbon* 1980, 18, 347.
- (116) Juntgen, H.; Knoblauch, K.; Reichenberger, J. Heimbach, H.; Tarnow, F. U.S. Patent 4 263 339, 1981.
- (117) Lemcoff, N. C.; Gmelin, R. C. U.S. Patent 5 176 722, 1993.
- (118) Cabrera, A. L.; Armor, J. N. U.S. Patent 5 071 450, 1991.
- (119) Sircar, S.; Golden, T. C.; Rao, M. D. *Carbon* 1996, 34, 1.
- (120) Armor, J. N.; Farris, T. S. *Extended Abstracts, 'Carbon '94'*, Granada, Spain, 1994; p 324.
- (121) Rao, M. B.; Sircar, S. *J. Membrane Sci.* 1993, 85, 253.
- (122) Tenison, S.R. *Extended Abstracts, 'Carbon '96'*, Newcastle upon Tyne, UK, 1996; p 541.
- (123) Suzuki, M. *Carbon* 1994, 32, 577
- (124) Burchell, T. D.; Judkins, R. R. *Energy Convers. Mgmt.* 1996, 37, 947.
- (125) Wilson, A. M.; Dahn, J. R. *J. Electrochem. Soc.* 1995, 142, 326.
- (126) Zheng, T.; Dahn, J. R. *Synthetic Metals* 1995, 73, 1.
- (127) Dahn, J. R.; Zheng, T.; Liu, Y. H.; Xue, J. S. *Science* 1995, 270, 590.
- (128) Zheng, T.; Xue, J. S.; Dahn, J. R. *Chem. Mater.* 1995, 8, 389.
- (129) Liu, Y. H.; Xue, J. S.; Zheng, T.; Dahn, J. R. *Carbon* 1996, 34, 193.
- (130) Winans, R. E.; Carrod, K. A. *J. Power Sources* 1995, 54, 11.
- (131) Sandi, G.; Carrado, K. A.; Winans, R. E.; Brenner, J. R.; Zajac, G. W. In *Microporous and Macroporous Materials*; Lobo, R. F.; Beck, J. S.; Suib, S. L.; Corbin, D. R.; Davis, M. E.; Iton, L. E.; Zones, S. I. Eds.; MRS Symp. Proc.; Materials Research Society: Pittsburgh, PA, 1996; Vol. 431, p 39.

- (132) Winans, R. E.; Carrado, K. A.; Thiyagaran, P.; Sandi, G.; Hunt, J. E.; Zajac, G. W. *Preprints to the 22nd Biennial Conference on Carbon*, 1995.
- (133) Iler, R. K. *The Chemistry of Silica*; Wiley: New York, 1979; Chapter 3.
- (134) Satterfield, C. N. *Heterogeneous Catalysis in Practice*; McGraw-Hill: New York, 1980; pp 92-93.
- (135) Reference 133, pp 578-599.
- (136) Brinker, C. J.; Scherer, G. W. *Sol-Gel Science*; Academic: New York, 1990.
- (137) Jones, R. W. *Fundamental Principles of Sol-Gel Technology*; The Institute of Metals: London, 1989.
- (138) *Better Ceramics Through Chemistry VII: Organic/Inorganic Hybrid Materials*; Coltrain, B. K., Sanchez, C., Schaefer, D. W., Wilkes, G. L. Eds.; MRS Symp. Proc.; Materials Research Society: Pittsburgh, PA 1996; Vol. 435.
- (139) Reference 136, pp 521-526.
- (140) Brinker, C. J.; Drotning, W. D.; Scherer, G. W. In *Better Ceramics Through Chemistry*; Brinker, C. J., Clark, D. E., Ulrich, D. R. Eds.; Elsevier: New York, 1984; p 25.
- (141) (a) Ramsay, J. D. F.; Avery, R. G. *Br. Ceram. Proc.* **1986**, *38*, 275. (b) Lecloux, A. J.; Bronckart, J.; Noville, F.; Dodet, C.; Marchot, P.; Pirard, J. P. *Colloids Surf.* **1986**, *19*, 359.
- (142) Martin, J. E.; Wilcoxon, J. P. *Phys. Rev. A* **1989**, *39*, 252.
- (143) Martin, J. E.; Adolf, D. *Annu. Rev. Phys. Chem.* **1991**, *42*, 311.
- (144) Martin, J. E.; Odinek, J. *Macromolecules* **1990**, *23*, 3362.
- (145) Reference 136, pp 160-174.
- (146) Reference 136, Chapter 6.
- (147) Hæreid, S.; Dahle, M.; Lima, S.; Einarsrud, M. A. *J. Non-Cryst. Solids* **1995**, *186*, 96.
- (148) Hæreid, S.; Anderson, J.; Einarsrud, M. A.; Hua, D. W.; Smith, D. M. *J. Non-Cryst. Solids* **1995**, *185*, 221.

- (149) S. Wallace, C. J. Brinker, and D. M. Smith, In *Advances in Porous Materials*; Komarneni, S., Smith, D. M., Beck, J. S. Eds.; MRS Symp. Proc.; Materials Research Society: Pittsburgh, PA, 1995; Vol. 371, p 241.
- (150) Scherer, G. W.; Smith, D. M. *J. Non-Cryst. Solids* 1995, 189, 197.
- (151) Fahrenholtz, W. G.; Smith, D. M. In *Better Ceramics Through Chemistry V*; Hampden-Smith, M. J., Klemperer, W. G., Brinker, C. J. Eds.; MRS Symp. Proc.; Materials Research Society: Pittsburgh, 1992; Vol. 271, p 705.
- (152) Banks, W. H.; Barkas, W. W. *Nature*, 1946, 158, 341.
- (153) Raman, N. K.; Anderson, M. T.; Brinker, C. J. *Chem. Mater.* 1996, 8, 1682.
- (154) Smith, D. M.; Deshpande, R.; Brinker, C.J. In *Better Ceramics Through Chemistry V*; Hampden-Smith, M. J., Klemperer, W. G., Brinker, C. J. Eds.; MRS Symp. Proc.; Materials Research Society: Pittsburgh, 1992; Vol. 271, p 567.
- (155) Prakash, S. S.; Brinker, C. J.; Hurd, A. J.; Rao, S. M. *Nature* 1995, 374, 439.
- (156) Reference 136, Chapter 9.
- (157) Reference 136, Chapter 11.
- (158) Scherer, G. W. *J. Sol-Gel Sci. Tech.* 1997, 8 , 353.
- (159) Klemperer, W. G.; Mainz, V. V. In *Better Ceramics Through Chemistry II*; Brinker, C. J., Clark, D. E., Ulrich, D. R. Eds.; MRS Symp. Proc.; Materials Research Society: Pittsburgh, 1986; Vol. 73, p 3.
- (160) Klemperer, W. G.; Mainz, V. V.; Millar, D. M. In *Better Ceramics Through Chemistry II*, Brinker, C. J., Clark, D. E., Ulrich, D. R. Eds; MRS Symp. Proc.; Materials Research Society: Pittsburgh, PA, 1986; Vol. 73, p 15.
- (161) Day, V. W.; Klemperer, W. G.; Mainz, V. V.; Millar, D. M. *J. Am. Chem. Soc.* 1985, 107, 8262.
- (162) Schmidt, R.; Mosset, A.; Galy, J. J. *Chem. Soc., Dalton Trans.* 1991, 1999.

- (163) Klemperer, W. G.; Ramamurthy, S. D. In *Better Ceramics Through Chemistry III*; Brinker, C. J., Clark, D. E., Ulrich, D. R. Eds.; MRS Symp. Proc.; Materials Research Society: Pittsburgh, PA, 1988; Vol. 121, p 1.
- (164) Klemperer, W. G.; Mainz, V. V.; Ramamurthy, S. D.; Rosenberg, F. S. In *Better Ceramics Through Chemistry III*; Brinker, C. J.; Clark, D. E.; Ulrich, D. R., Eds.; MRS Symp. Proc.; Materials Research Society: Pittsburgh, PA, 1988; Vol. 121, p 15.
- (165) Klemperer, W. G.; Ramamurthy, S. D. *J. Noncryst. Sol.* **1990**, *121*, 16.
- (166) Cagle, P. C.; Klemperer, W. G.; Simmons, C. A. In *Better Ceramics Through Chemistry IV*; Zelinski, B. J. J., Brinker, C. J., Clark, D. E., Ulrich, D. R. Eds.; MRS Symp. Proc.; Materials Research Society: Pittsburgh, PA 1990; Vol. 180, p 29.
- (167) Chen, Y. W.; Klemperer, W. G.; Park, C. W. In *Better Ceramics Through Chemistry V*; Hampden-Smith, M. J., Klemperer, W. G., Brinker, C. J. Eds.; MRS Symp. Proc.; Materials Research Society: Pittsburgh, PA, 1992; Vol. 271, p 57.
- (168) Chen, Y. W.; Klemperer, W. G. submitted for publication.
- (169) Avnir, D.; Klein, L. C.; Levy, D.; Schubert, U.; Wojcik, A. B. In *The Chemistry of Organic Silicon Compounds*; Rappoport, Z., Apeloig, Y. Eds.; Wiley: New York, 1998; Volume 2, Chapter 40.
- (170) (a) Reetz, M. T.; Zonta, A.; Simpelkamp, J. *Angew. Chem. Int. Ed. Engl.* **1995**, *34*, 301. (b) Wheeler, G. E.; Fleming, S. A. In *Ultrastructure Processing of Advanced Materials*; Uhlmann, D. R., Ulrich, D. R. Eds.; Wiley: New York, 1992; p. 327.
- (171) Devreux, F.; Boilot, J. P.; Chaput, F. *Phys. Rev. A.* **1990**, *41*, 6901.
- (172) Baney, R. H.; Itoh, M.; Sakakibara, A.; Susuki, T. *Chem. Rev.* **1995**, *95*, 1409.
- (173) (a) Voronkov, M. G., Lavrent'yev, V. I. *Top. Curr. Chem* **1982**, *102*, 199. (b) Brown, J. F., Jr.; Vogt, L. H., Jr.; Prescott, P. I. *J. Am. Chem. Soc.* **1964**, *86*, 1120.
- (174) (a) Slinyakova, I. B.; Kurennaya, L. I. *Vysokomol. Soedin., Ser. B.* **1972**, *14*, 889. (b) Andrianov, K. A.; Slonimskii, G. L.; Zhdanov, A. A.; Tsvankin, D. Ya., Levin, V. Yu.,

- Papkov, V. S.; Kvachev, Yu. P.; Belavtseva, E. M. *J. Polym. Sci., Polym. Chem. Ed.* 1976, 14, 1205.
- (175) Zimmer, I. A.; Aristova, V. G.; Galitskaya, O. A.; Gorbunov, A. I.; Sobolevskii, M. V.; Grinevich, K. P.; Romanova, I. P. *USSR Plast. Massy* 1976, 1, 50.
- (176) (a) Loy, D. A.; Shea, K. J. *Chem. Rev.* 1995, 95, 1431. (b) Corriu, R. J. P.; Leclercq, D. *Angew. Chem. Int. Ed. Engl.* 1996, 35, 1420.
- (177) Shea, K. J.; Loy, D. A.; Webster, O. *J. Am. Chem. Soc.* 1992, 114, 6700.
- (178) Martino, A.; Yamanaka, S. A.; Kawola, J. S.; Loy, D. A. *Chem. Mater.* 1997, 9, 423.
- (179) Loy, D. A.; Russick, E. M.; Yamanaka, S. A.; Baugher, B. M.; Shea, K. J. *Chem. Mater.* 1997, 9, 2264.
- (180) Loy, D. A.; Carpenter, J. P.; Myers, S. A.; Assink, R. A.; Small, J. H.; Greaves, J.; Shea, K. J. *J. Am. Chem. Soc.* 1996, 118, 8501.
- (181) McClain, M. D.; Loy, D. A.; Prabakar, S. In *Better Ceramics Through Chemistry VII: Organic/Inorganic Hybrid Materials*; Coltrain, B. K., Sanchez, C., Schaefer, D. W., Wilkes G. L., Eds.; MRS Symp. Proc.; Materials Research Society: Pittsburgh, PA 1996; Vol. 435, p 33.
- (182) Loy, D. A.; Shea, K. J.; Russick, E. M. In *Better Ceramics Through Chemistry V*; Hampden-Smith, M. J., Klemperer, W. G., Brinker, C. J. Eds.; MRS Symp. Proc.; Materials Research Society: Pittsburgh, 1992; Vol. 271, p 699.
- (183) Loy, D. A.; Jamison, G. M.; Baugher, B. M.; Russick, E. M.; Assink, R. A.; Prabakar, S.; Shea, K. J. *J. Non Cryst. Solids* 1995, 186, 44.
- (184) (a) Small, J. H.; Shea, K. J.; Loy, D. A. *J. Non-Cryst. Solids* 1993, 160, 234. (b) Oviatt, H. W., Jr.; Shea, K. J.; Small, J. H. *Chem. Mater.* 1993, 5, 943.
- (185) Whitehurst, D. D.; Mitchell, T. O. German Patent 2 511 344, 1975.
- (186) (a) Loy, D. A.; Buss, R. J.; Assink, R. A.; Shea, K. J.; Oviatt, H. *Polym. Prepr.* 1993, 34, 244. (b) Loy, D. A.; Shea, K. J.; Buss, R. J.; Assink, R. A. In *Inorganic, and*

- Organometallic Polymers II*; Wisian-Neilson, P., Allcock, H. R., Wynne, K. J. Eds.; ACS Symposium Series 572; American Chemical Society: Washington, DC, 1994; p 122.
- (187) Nakanishi, K. Takahashi, R.; Soga, H. *J. Non-Cryst. Solids* 1992, 147&148, 291.
- (188) (a) Schubert, U.; Husing, N.; Lorenz, A. *Chem. Mater.* 1995, 7, 2010. (b) Schubert, U. *New J. Chem.* 1994, 18, 1049.
- (189) Corriu, R. J. P.; Moreau, J. J. E.; Thepot, P.; Man, M. W. C. *J. Mater. Chem.* 1994, 4, 987.
- (190) Corriu, R. J. P.; Moreau, J. J. E.; Thepot, P.; Wong Chi Man, M.; *Chem. Mater.* 1992, 4, 1217.
- (191) Carpenter, J. P.; Yamanaka, S. A.; McClain, M. D.; Loy, D. A.; Greaves, J.; Hobson, S.; Shea, K. unpublished results.
- (192) Reference 1, pp 200-201.
- (193) Okuhara, T.; Mizuno, N.; Misono, M. *Adv. Catal.* 1996, 41, 113.
- (194) Izumi, Y.; Urabe, K.; Onaka, M. *Zeolite, Clay, and Heteropoly Acid in Organic Reactions*; VCH: Weinheim, 1992.
- (195) Misono, M.; Nojiri, N. *Appl. Catal.* 1990, 64, 1.
- (196) Reference 193, p 124.
- (197) Okuhara, T.; Tatematsu, S.; Lee, K. Y.; Misono, M. *Bull. Chem. Soc. Jpn.* 1989, 62, 717.
- (198) Lee, K. Y.; Arai, T.; Nakata, S.; Asaoka, S.; Okuhara, T.; Misono, M. *J. Am. Chem. Soc.* 1992, 114, 2836.
- (199) Hashimoto, M.; Misono, M. *Acta. Cryst.* 1994, C50, 231.
- (200) Okuhara, T.; Nishimura, T.; Misono, M. In *11th International Congress on Catalysis - 40th Anniversary*; Hightower, J. W., Delgass, W. N., Iglesia, E., Bell, A. T. Eds.; Studies in Surface Science and Catalysis 101; Elsevier: Amsterdam, 1996; p 581.

- (201) (a) Okuhara, T.; Nishimura, T.; Misono, M. *Chem. Lett.* 1995, 155; (b) Nishimura, T. Ph.D. Thesis, Univ. of Tokyo, 1995.
- (202) Inumaru, K.; Nakajima, H.; Ito, T.; Misono, M. *Chem. Lett.* 1996, 559; 1997, 727.
- (203) Pellenq, R. J-M.; Nicholson, D. *J. Phys. Chem.* 1994, 98, 13339.
- (204) Madden, W. G.; Glandt, E. D. *J. Stat. Phys.* 1988, 51, 537.
- (205) (a) Given, J. A.; Stell, G. *J. Chem. Phys.* 1992, 97, 4573. (b) Vega, C.; Kaminsky, R. D.; Monson, P. A. *J. Chem. Phys.* 1993, 99, 3003. (c) Lomba, E.; Given, J. A.; Stell, G.; Weis, J-J.; Levesque, D. *Phys. Rev. E* 1993, 48, 233. (d) Rosinberg, M. L.; Tarjus, G.; Stell, G. *J. Chem. Phys.* 1994, 100, 5172.

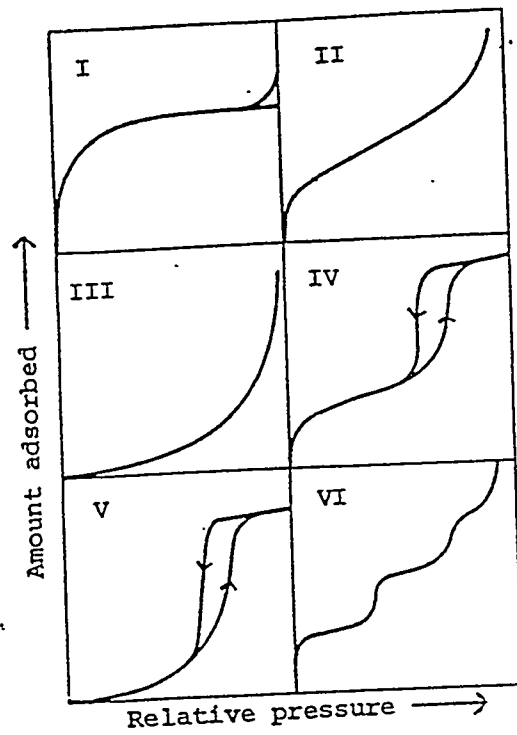


Figure 1

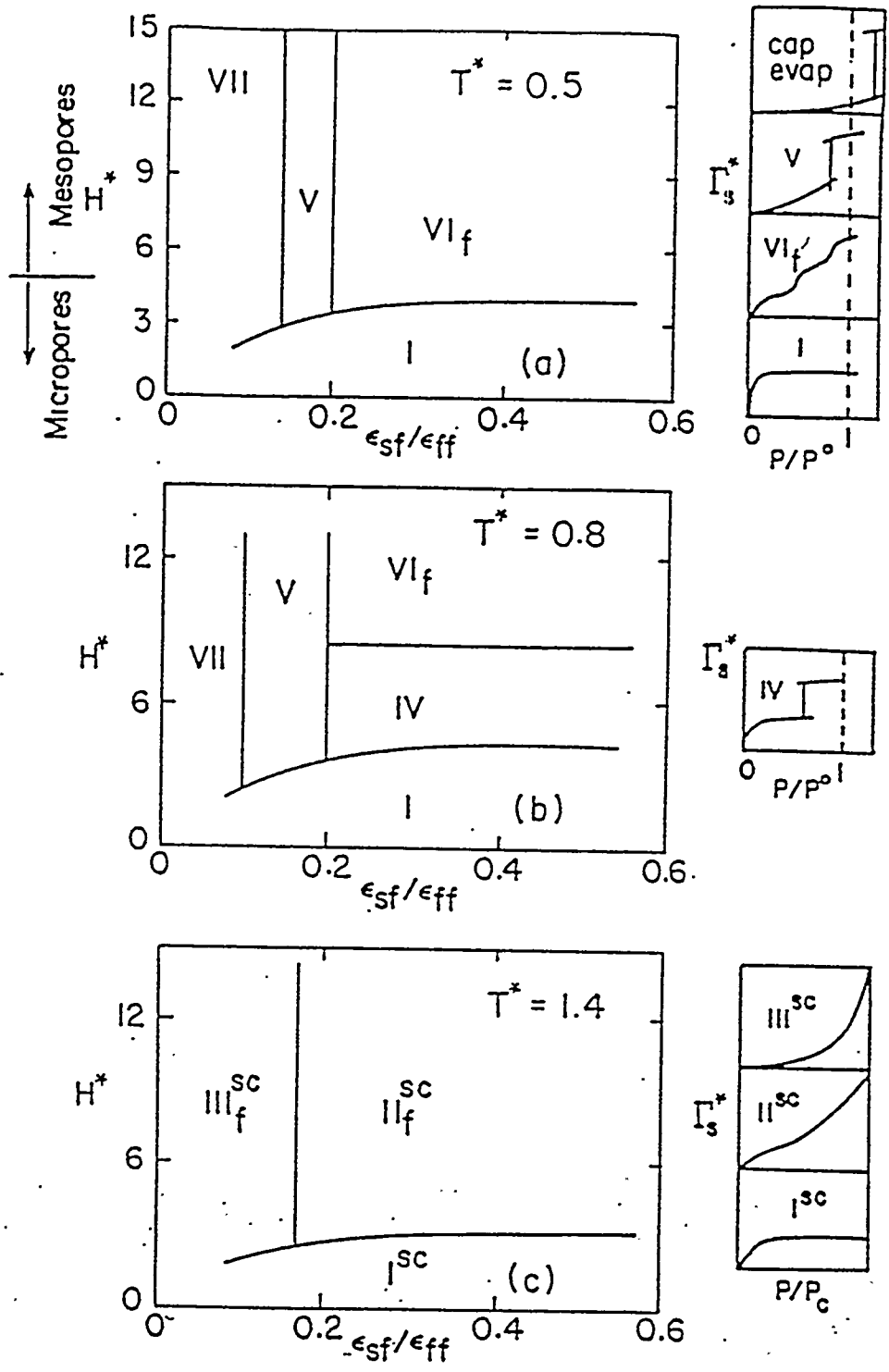
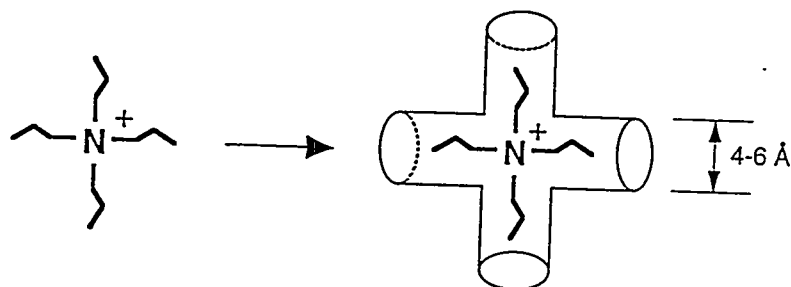
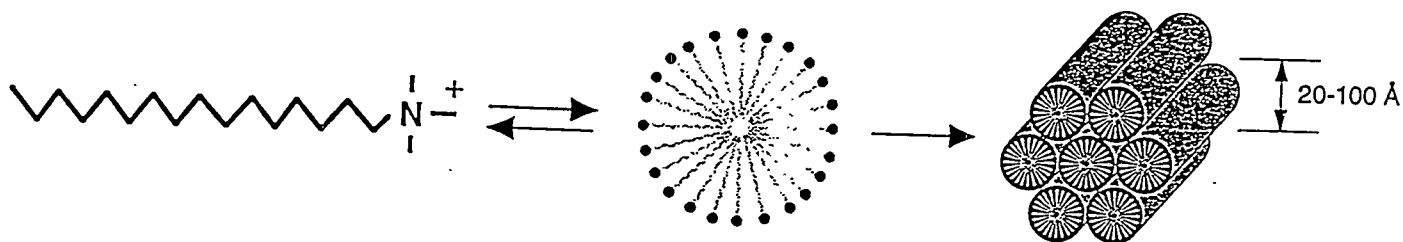


Figure 2

The Role of Quaternary Directing Agents



Individual Small Alkyl Chain Length Quaternary Directing Agents
Generate the Formation of Microporous Molecular Sieves

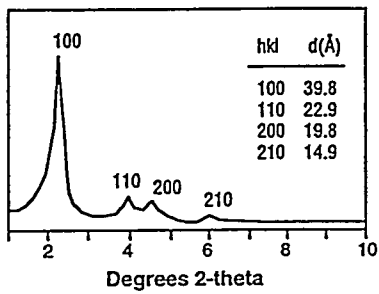


Long-Alkyl Chain Length Quaternary Directing Agents Self-Assemble to Supramolecular
Species Which Can Generate the Formation of Mesoporous Molecular Sieves

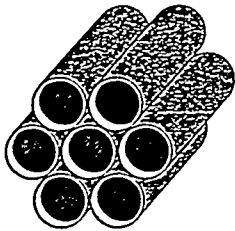
Figure 3

**MCM-41
(Hexagonal)**

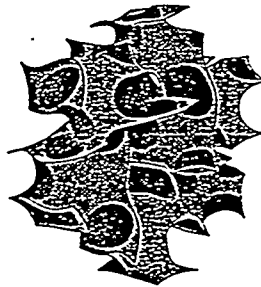
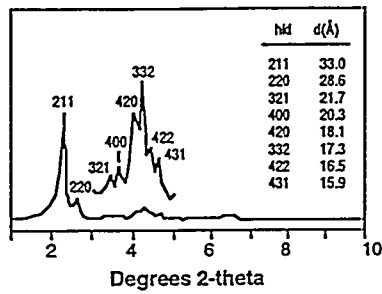
*X-ray
Diffraction
Pattern*



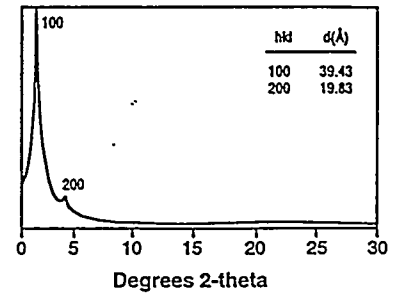
*Possible
Structures*



**MCM-48
(Cubic)**



**MCM-50
(Stabilized Lamellar)**



Silica
Sheets

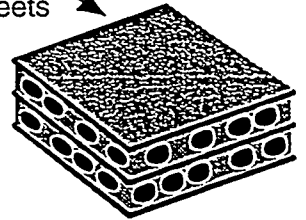
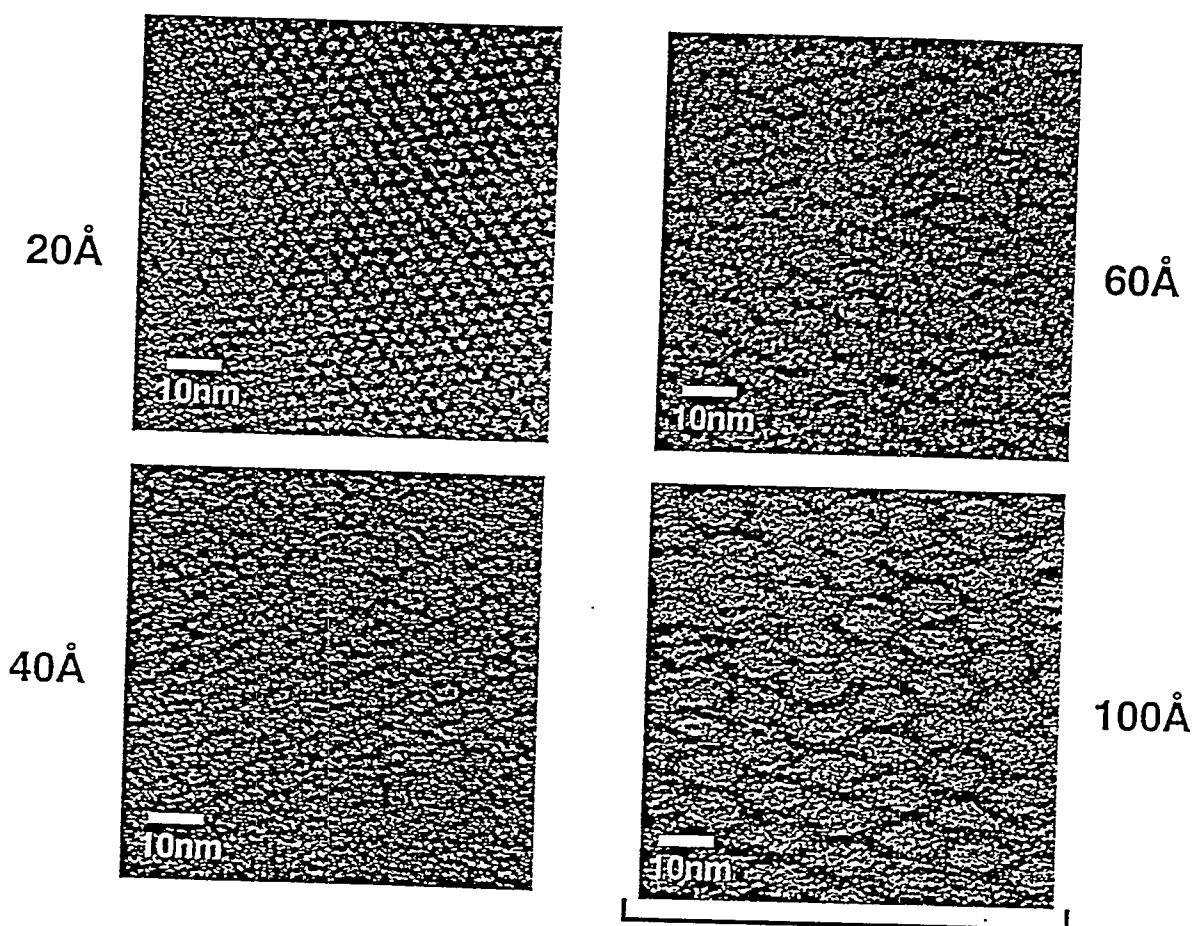


Figure 4



Prepared with Mesitylene Addition

Figure 5

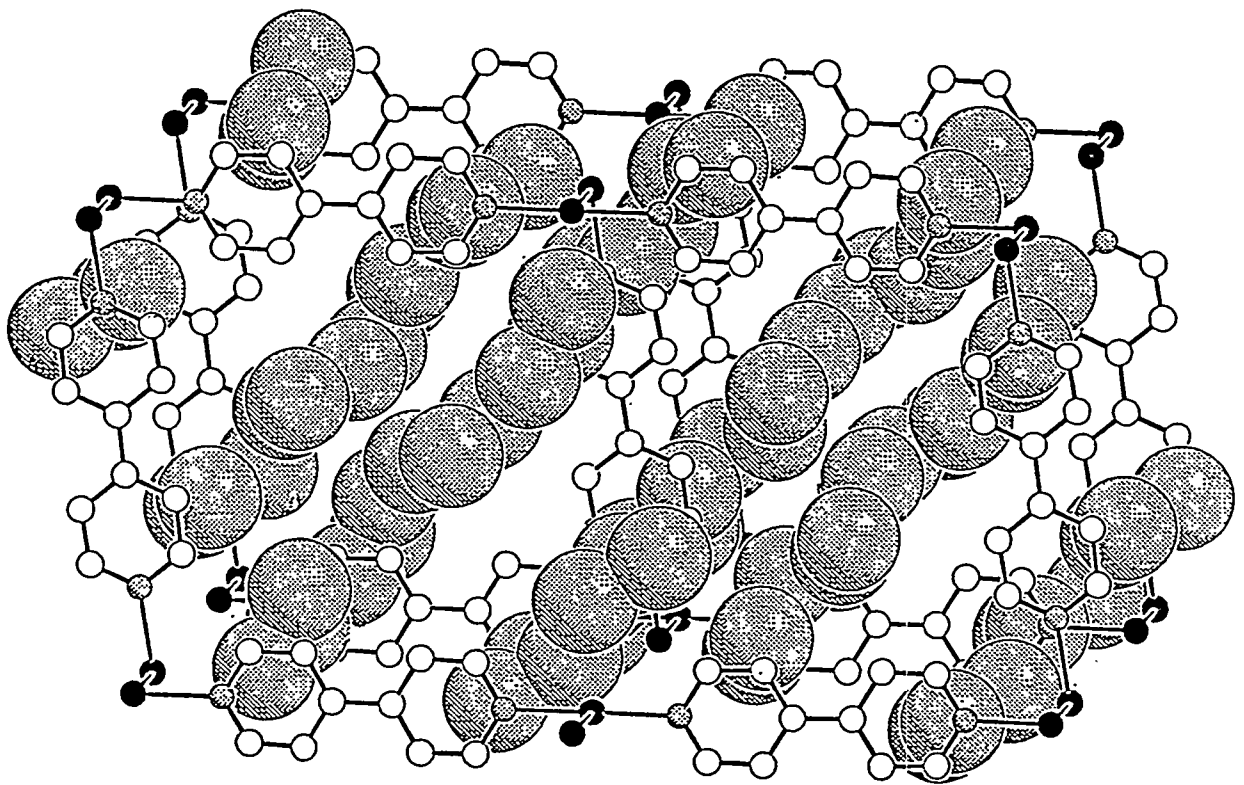


Figure 6

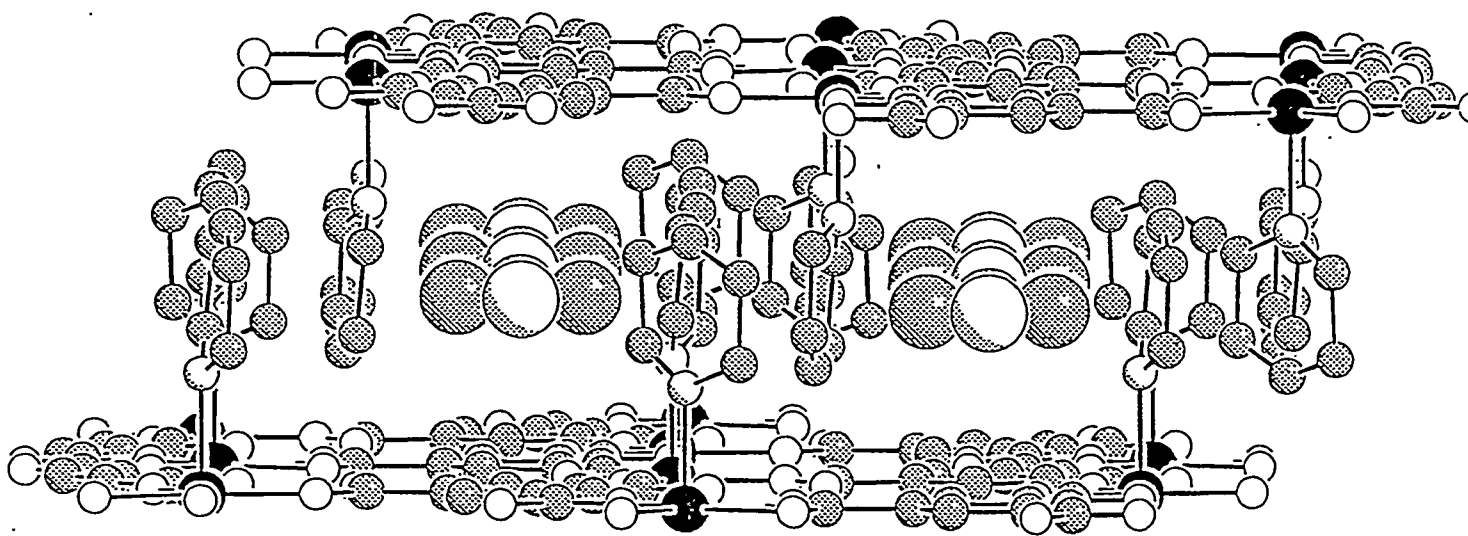


Figure 7

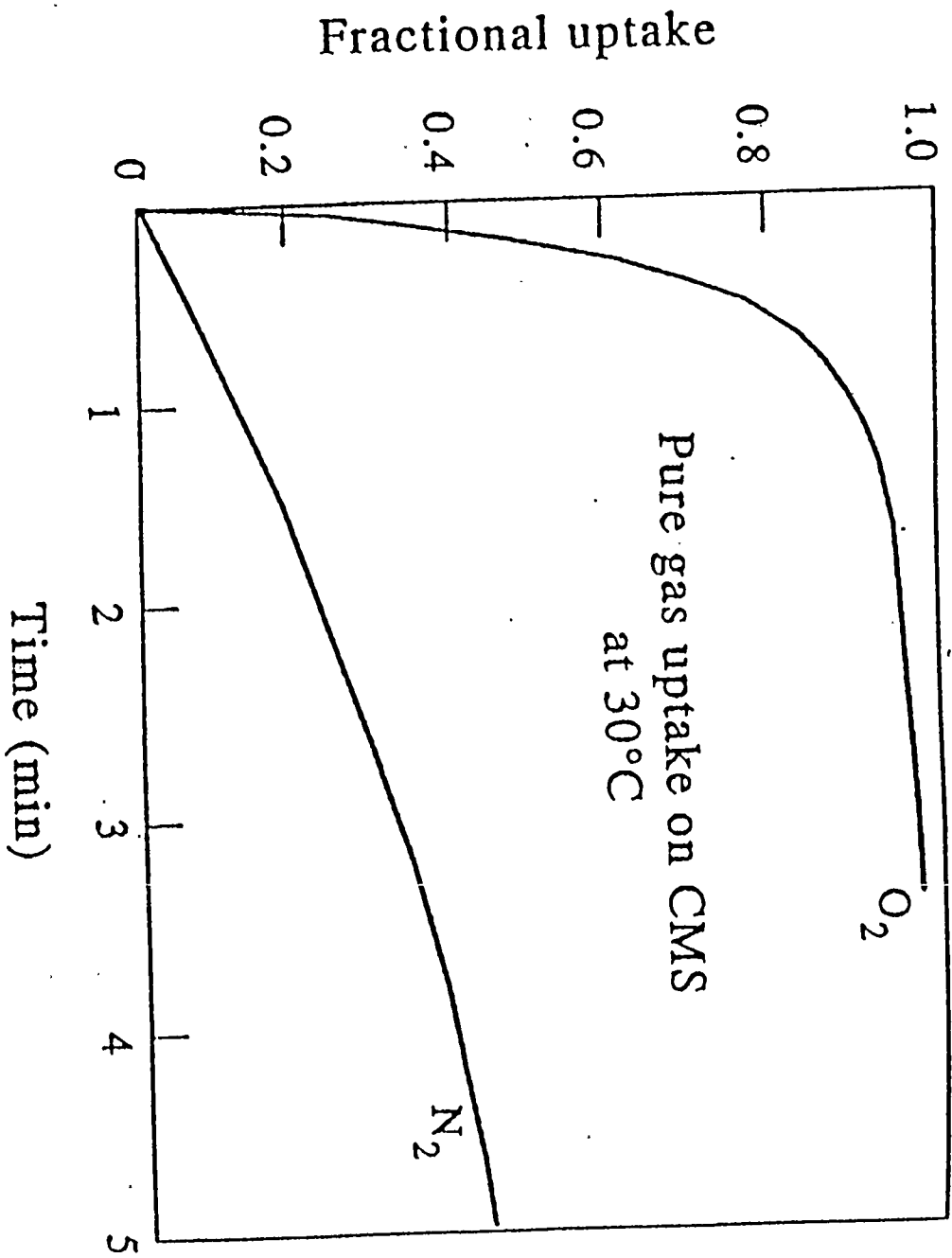


Figure 8

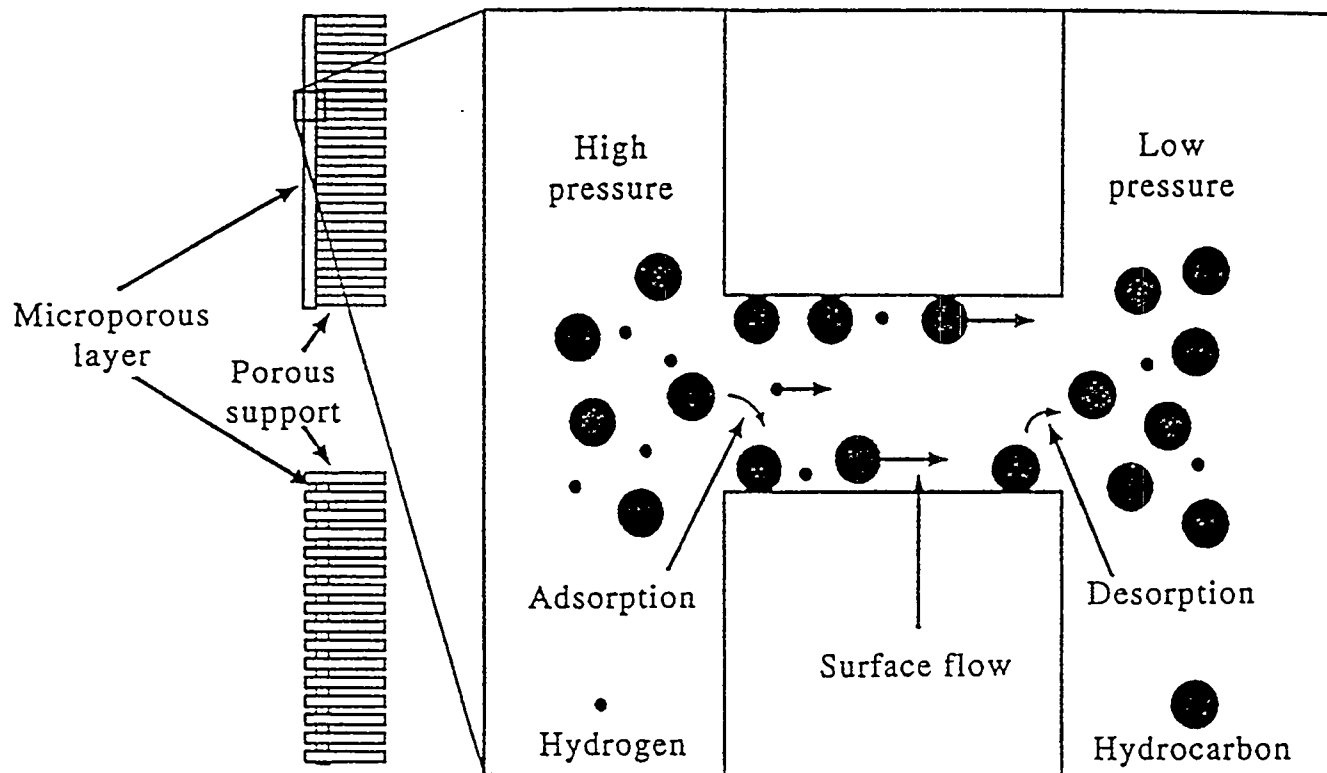


Figure 9

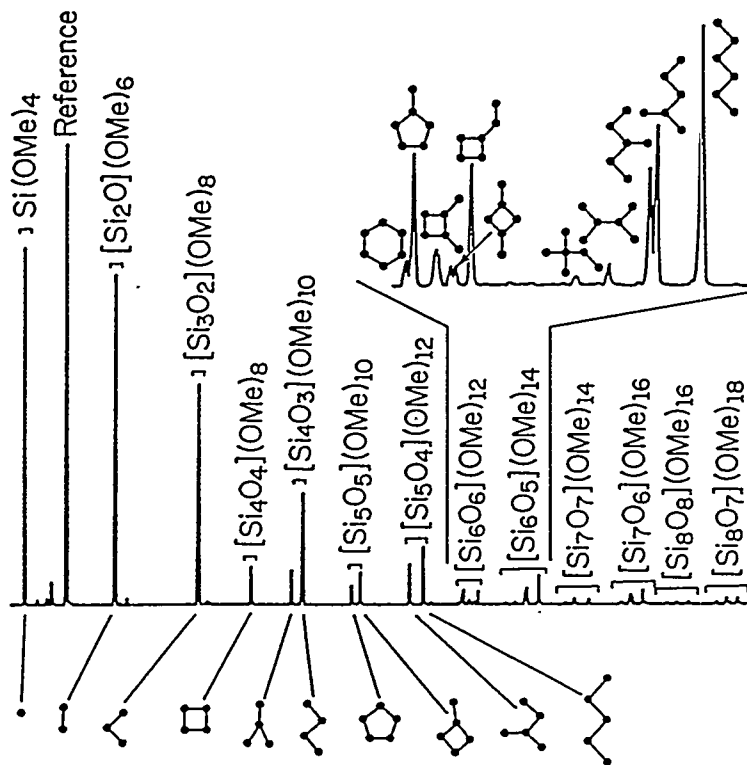
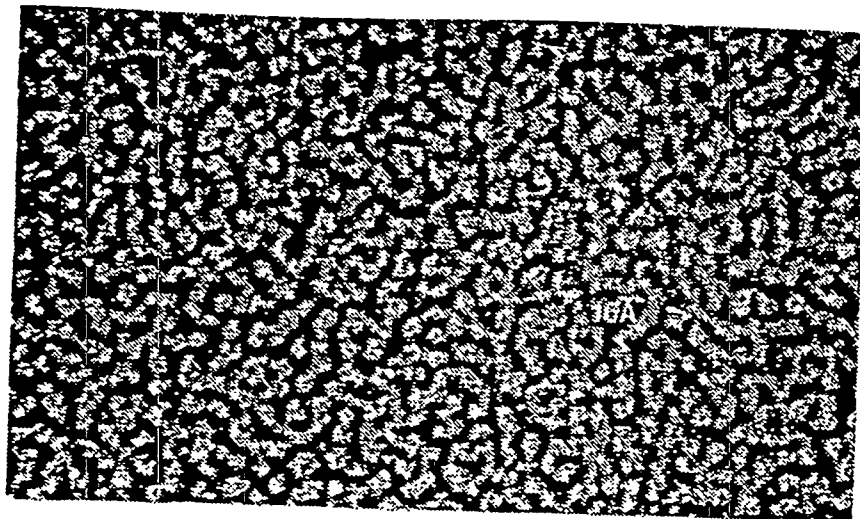


Figure 10

a)



b)

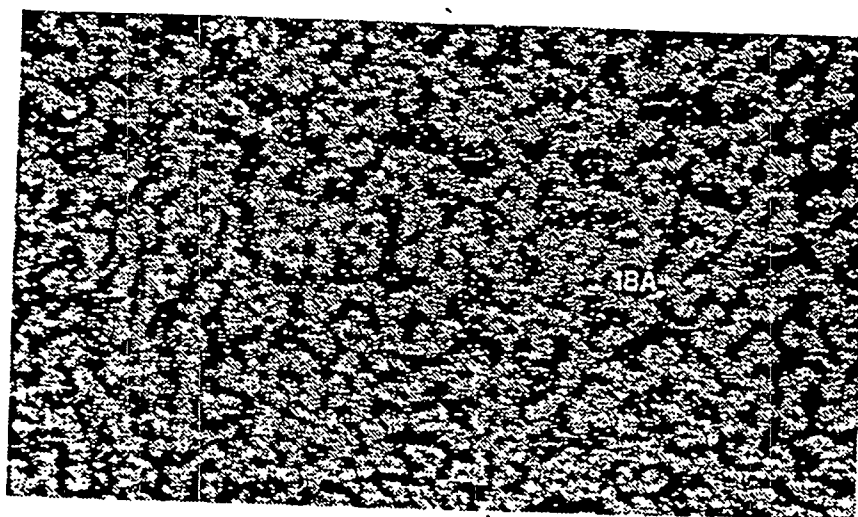


Figure 11.

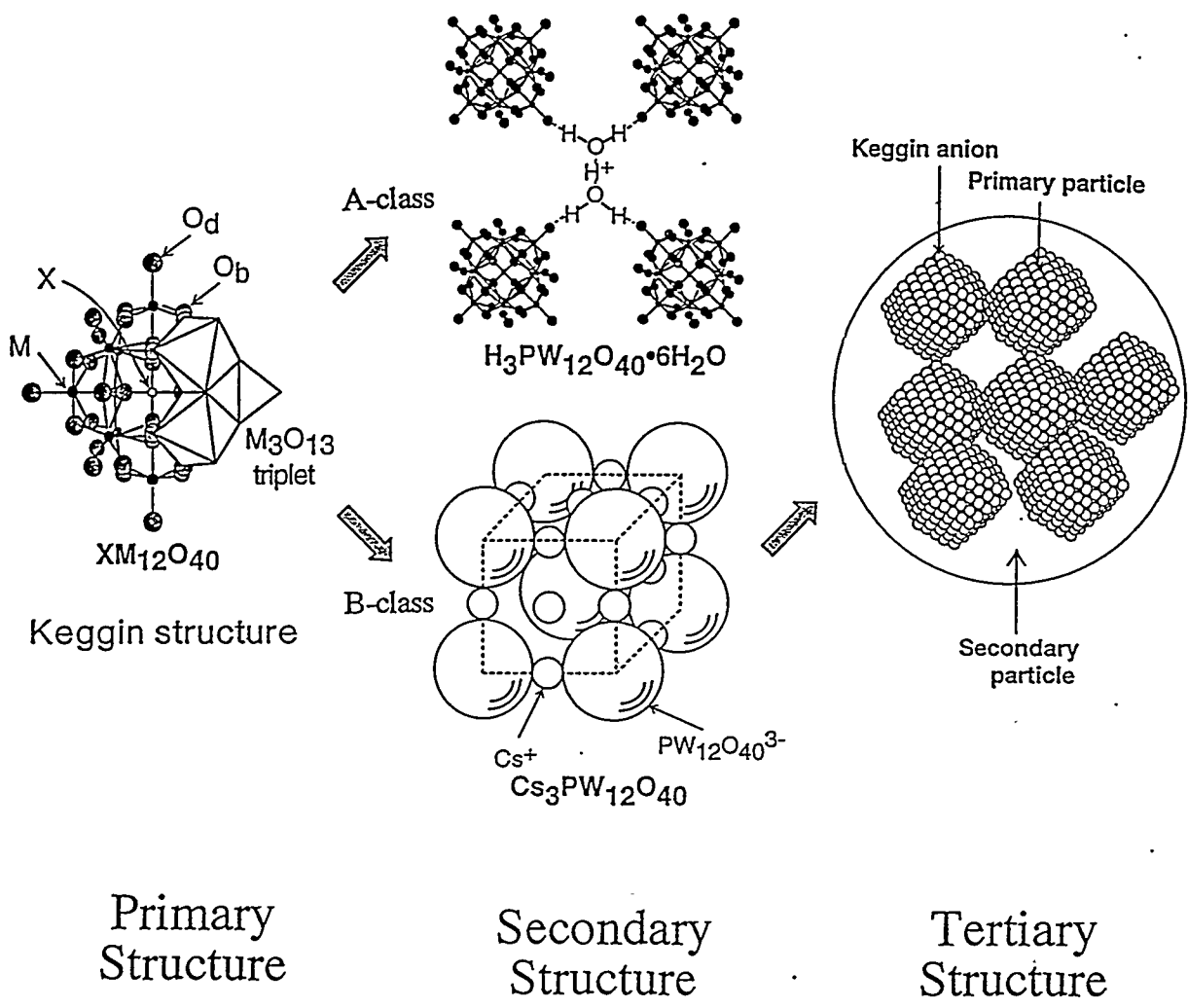


Figure 12

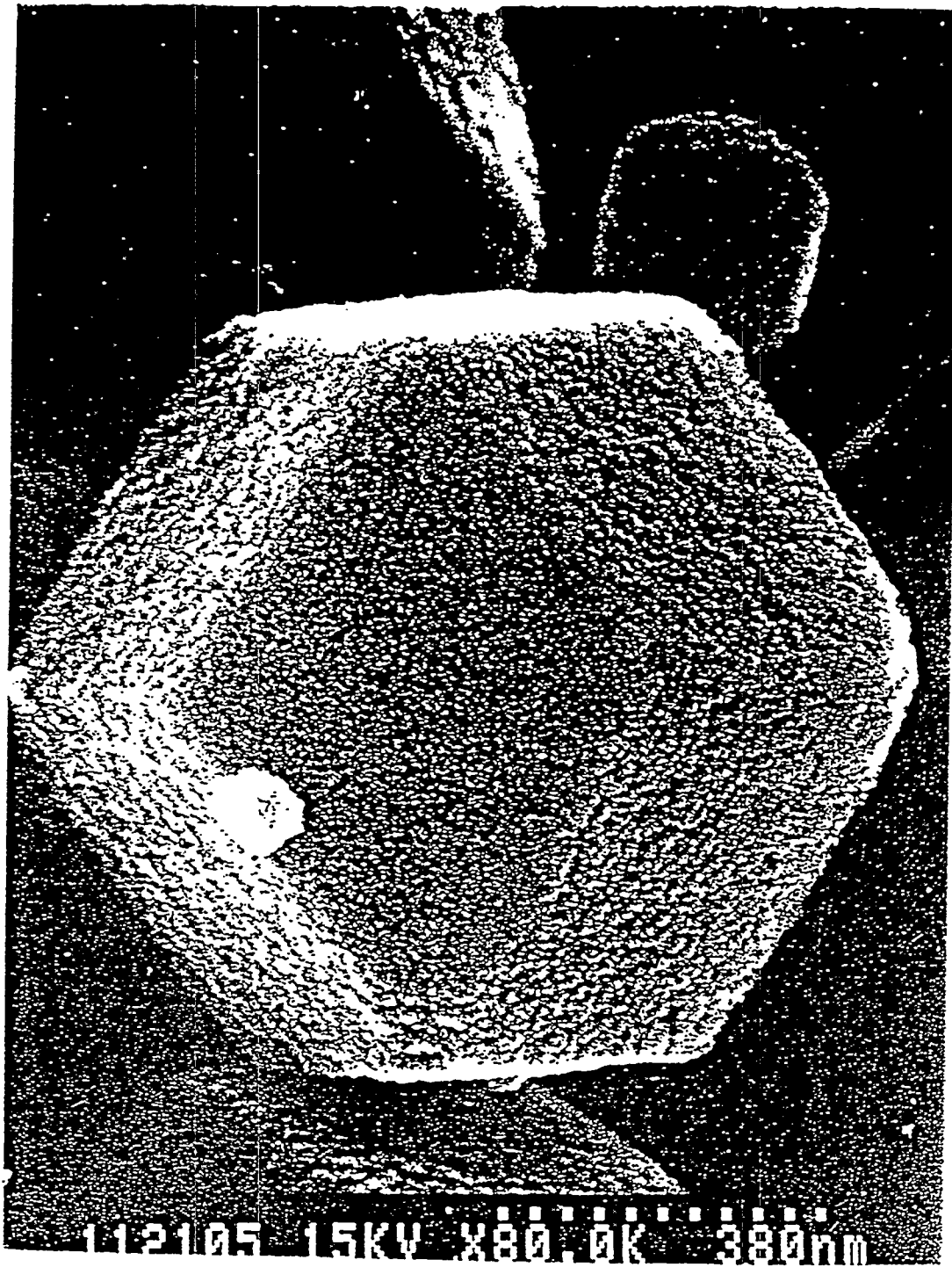
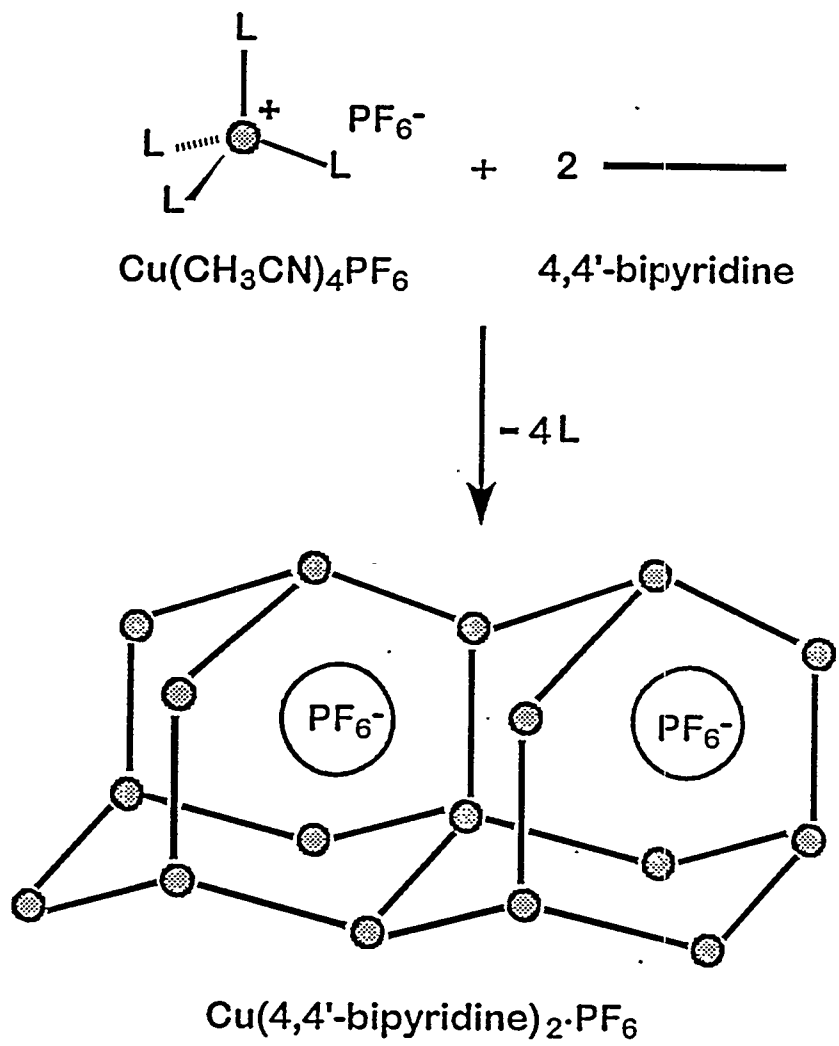
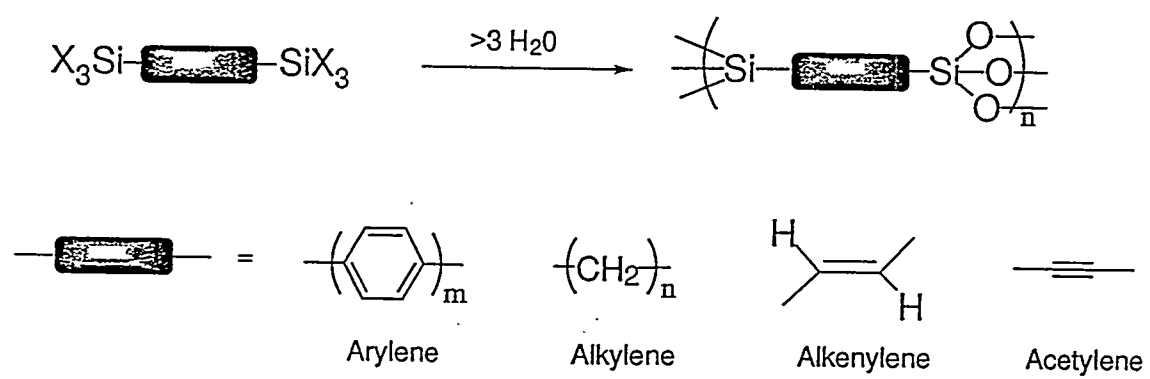


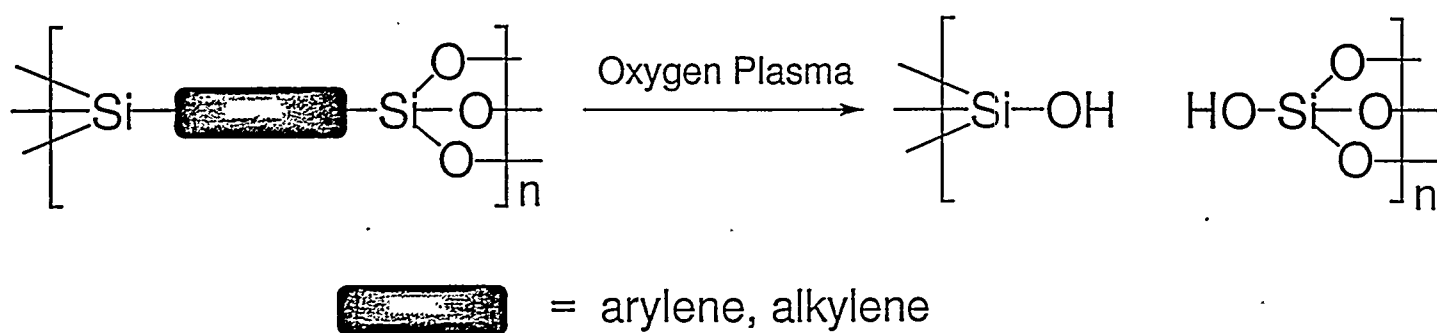
Figure 13



Scheme 1



Scheme 2



Scheme 3